CANCER

PAX5 epigenetically orchestrates CD58 transcription and modulates blinatumomab response in acute lymphoblastic leukemia

Yizhen Li[1], Takaya Moriyama[1], Satoshi Yoshimura[1], Xujie Zhao[1], Zhenhua Li[1], Xu Yang[2], Elisabeth Paietta[3], Mark R. Litzow[4], Marina Konopleva[5], Jiyang Yu[2], Hiroto Inaba[6], Raul C. Ribeiro[6], Ching-Hon Pui[6], Jun J. Yang[1]*

Blinatumomab is an efficacious immunotherapeutic agent in B cell acute lymphoblastic leukemia (B-ALL). However, the pharmacogenomic basis of leukemia response to blinatumomab is unclear. Using genome-wide CRISPR, we comprehensively identified leukemia intrinsic factors of blinatumomab sensitivity, i.e., the loss of CD58 as a top driver for resistance, in addition to CD19. Screening 1639 transcription factor genes, we then identified PAX5 as the key activator of CD58. ALL with the PAX5 P80R mutation also expressed the lowest level of CD58 among 20 ALL molecular subtypes in 1988 patients. Genome editing confirmed the effects of this mutation on CD58 expression and blinatumomab sensitivity in B-ALL, with validation in patient leukemic blasts. We described a PAX5-driven enhancer at the CD58 locus, which was disrupted by PAX5 P80R, and the loss of CD58 abolished blinatumomab-induced T cell activation with global changes in transcriptomic/epigenomic program. In conclusion, we identified previously unidentified genetic mechanisms of blinatumomab resistance in B-ALL, suggesting strategies for genomics-guided treatment individualization.

INTRODUCTION

Blinatumomab is a bispecific molecule that engages CD3+ T cells with CD19-expressing malignant B cells, thus inducing tumor lysis by T cell immune response (1, 2). This direct coupling can rapidly activate T cell receptor (TCR) signaling and initiates a polyclonal T cell response, circumventing major histocompatibility complex restriction and TCR epitope selectivity, which are otherwise required for the development of tumor-specific cytotoxic T cells (3, 4). In pediatric and adult B cell acute lymphoblastic leukemia (B-ALL), blinatumomab exhibited remarkable efficacy even in patients with relapsed or refractory diseases (1, 5–10). For example, a recent Children's Oncology Group randomized trial of 208 children with relapsed B-ALL showed that two cycles of blinatumomab immediately after chemotherapy-based induction therapy produced a 2-year disease-free survival of 54.4% compared to 39.0% in those receiving conventional chemotherapy as consolidation therapy. The first cycle of blinatumomab induced minimal residual disease (MRD)–negative remission in 75% of the patients, whereas conventional consolidation chemotherapy achieved MRD-negative status in only 32% of the patients (5). Blinatumomab also improved the outcome of patients with refractory disease and positive MRD after intensive remission induction treatment, prompting the recent expansion of blinatumomab indication to MRD+ ALL (11–14). In adult ALL, several groups have now explored blinatumomab-based combination or sequential therapies with other targeted

agents (15–17). For example, a chemotherapy-free regimen featuring up to five cycles of blinatumomab plus daily ponatinib produced a 1-year overall survival rate of 94% in adults with breakpoint cluster region-Abelson (BCR-ABL1) ALL (18). These paradigm-shifting treatment regimens represent prototypes of "chemo-free" therapy for ALL, pointing to blinatumomab as a potentially critical component of the next generation of ALL therapy in the near future.

While large frontline ALL trials of blinatumomab are lacking, existing data strongly indicate substantial interpatient variability in response and toxicities. Complete remission rate ranges from 36 to 66%, depending on the regimen used (the number of cycles, timing, and concomitant antileukemic agents) and patient characteristics (age and ALL subtype) (19–22). Moreover, the duration of remission varies among trials, with a notableproportion of patients experiencing relapse or progressive disease following blinatumomab treatment, raising concerns about acquired drug resistance. For patients relapsed on blinatumomab, it is estimated that 36.4% is due to the loss of CD19 antigen on B-ALL blasts as a result of nonsense or frameshift mutations or genomics aberrations affecting alternative splicing at the CD19 locus (23). Mechanisms of resistance in CD19+ relapse remain largely unclear, although many hypotheses have been proposed, including T cell exhaustion, CD19 trafficking, and adaptive immune escape Programmed Cell Death Protein 1 (PD-1)- or Programmed Cell Death Ligand 1 (PD-L1)–mediated] (3, 24–26). With the growing usage of blinatumomab therapy, it is imperative to identify molecular determinants of drug response and develop strategies to forestall the emergence of resistance.

In this study, we performed a genome-wide CRISPR screen to systematically characterize leukemia intrinsic drivers of blinatumomab resistance. Focusing on one of the top hits, namely, CD58, we performed a series of functional studies to describe the molecular mechanism by which CD58 regulates B-ALL sensitivity to

[1]Division of Pharmaceutical Sciences, Department of Pharmacy and Pharmaceutical Sciences, St. Jude Children's Research Hospital, Memphis, TN, USA. [2]Department of Computational Biology, St. Jude Children's Research Hospital, Memphis, TN, USA. [3]Montefiore Medical Center, Bronx, NY, USA. [4]Division of Hematology, Department of Internal Medicine, Mayo Clinic, Rochester, MN, USA. [5]Department of Leukemia, The University of Texas MD Anderson Cancer Center, Houston, TX, USA. [6]Department of Oncology, St. Jude Children's Research Hospital, Memphis, TN, USA.
*Corresponding author. Email: jun.yang@stjude.org

blinatumomab. We identified *PAX5* P80R mutation as the key leukemia genomic lesion linked to *CD58* down-regulation and hence blinatumomab resistance and further elucidated the epigenomic mechanism of Paired Box 5 (PAX5)-mediated *CD58* transcription regulation. Our study provided previously unidentified insights into the genomic basis of blinatumomab resistance in B-ALL with potential implications for individualized use of the immunotherapeutic agent in lymphoid malignancies.

RESULTS

Genome-wide CRISPR screen identifies *CD19, CD81,* and *CD58* as top ALL intrinsic factors related to blinatumomab resistance

To comprehensively identify genes involved in ALL responses to blinatumomab, we performed a genome-wide CRISPR screen in B-ALL cell line Nalm6 using a T cell coculture system. In this assay, Nalm6 cells harboring knockout of different genes were incubated with blinatumomab (1 or 100 ng/ml) in the presence of normal T cells for 7 days. B-ALL cells that survived blinatumomab treatment were considered as drug resistant, and we examined the enrichment of single guide RNAs (sgRNAs) targeting specific genes in this cell population relative to baseline (Fig. 1A). After excluding genes essential for Nalm6 survival, we identified 61 and 18 genes with sgRNA enriched at least twofold in blinatumomab-resistant cells and 10 and 74 genes with sgRNA depleted at least twofold in blinatumomab-resistant cells after exposure at 1 and 100 ng/ml, respectively (Fig. 1B). Five genes were common in both conditions: *CD19, CD81, CD58, DFFA,* and *DFFB* (Fig. 1, C and D). As expected, losing the CD19 antigen in B-ALL showed the greatest effect in blunting blinatumomab-induced T cell cytotoxicity. CD81 is a chaperone protein essential for CD19 surface presentation, and loss-of-function mutations in this gene have been linked to CD19-negative B-ALL relapse after blinatumomab therapy (*25, 27*). *DFFA* and *DFFB* encode proteins essential for DNA fragmentation during apoptosis, but their effects on blinatumomab sensitivity were not validated in independent CRISPR experiments (fig. S1). By contrast, CD58 is commonly expressed in malignant B cells, and its interaction with CD2 molecules on T cells is critical for initiating T cell immune response (*28, 29*). We reasoned that knocking out *CD58* was likely to disrupt B-ALL–T cell interaction, driving blinatumomab resistance, as observed from the CRISPR screen. Therefore, we elected to focus on *CD58* for the rest of this study to characterize molecular details of this novel mechanism of resistance to bispecific antibody therapy.

CD58 level in B-ALL modulates leukemia response to blinatumomab-induced T cell cytotoxicity

To validate the genome-wide CRISPR screen results, we first generated new sgRNAs for *CD58* in Nalm6 and established two single clones with biallelic frameshift mutations at this locus and thus a complete loss of CD58 protein (fig. S2, A and B). We also generated isogenic Nalm6 cells with *CD19* deletion as a reference (fig. S2, C and D). Across six blinatumomab concentrations and with T cell coculture for 24 hours, $CD58^{KO}$ Nalm6 cells showed minimal leukemia lysis, whereas wild-type (WT) cells underwent rapid apoptosis in a dose-dependent fashion (Fig. 1E). Longer exposure to blinatumomab (72 hours) resulted in greater leukemia killing (up to 90%; fig. S3), although we also observed some evidence of T

cell exhaustion [PD1 and T-cell immunoglobulin and mucin domain 3 (TIM3); figs. S4 and S5]. Nalm6 forms big cell clumps with T cells under blinatumomab treatment, while $CD58^{KO}$ reduces the cell clump size, indicating that CD58 influences the physical interaction of B-ALL cells with T cells by blinatumomab (fig. S6). The degree of blinatumomab resistance resulting from $CD58^{KO}$ was only slightly lower than that seen in $CD19^{KO}$ Nalm6 cells. Conversely, sensitivity to blinatumomab was largely restored when we reintroduced CD58 in the knockout Nalm6 cells by ectopic expression (Fig. 1F and fig. S2E), confirming that drug resistance was specifically driven by the loss of CD58. The importance of CD58 in blinatumomab response was further validated in Nalm6 and another B-ALL cell line, 697, by using CD58 or CD2 blocking antibody; both markedly blunted B-ALL cell response to blinatumomab in vitro (Fig. 1, G and H), again pointing to the CD2-CD58 axis as a key determinant of B-ALL sensitivity to this drug.

### CRISPR-Cas9 screening identified transcription factors that regulate CD58 and CD19 expression in ALL

Next, we sought to comprehensively identify transcription factors (TFs) that are responsible for regulating CD58 and CD19 expression in ALL. A CRISPR-Cas9 sgRNA library was used to target 1639 human TFs, with seven sgRNAs per gene and 100 nontargeting sgRNAs included as negative control (*30*). Three paralleled screens for both CD58 and CD19 were performed in Nalm6 cells stably expressing Cas9. Cells were transduced with lentiviral sgRNA library at low multiplicity of infection (MOI = 0.25) and then subjected to flow cytometry to select for the top 10% and bottom 10% of cells with the highest and lowest CD58 or CD19 expression. sgRNAs enriched in each pool were identified by sequencing (Fig. 2A). For CD58, there were 11 TFs enriched in the low-expression Nalm6 cell population [$P < 0.05$, $\log_2$ fold change < -1, robust ranking algorithm (RRA) score $< 1 \times 10^{-8}$], suggesting that these TFs are essential for CD58 transcription (Fig. 2B and table S1). The top 10 positive regulator TFs for CD58 include *RUNX1, PAX5,* and *BCL11A,* among others. (Fig. 2C and table S1). Conversely, we identified six negative regulator TFs for CD58 (sgRNA enriched in $CD58^{high}$ Nalm6 cells), including *CREB1, ANF148,* and *SPI1,* to name a few. ($P < 0.05$, $\log_2$ fold change > 1, RRA score $< 1 \times 10^{-8}$; Fig. 2D). For CD19, CRISPR screen identified nine positive regulator TFs, including *ZBTB7A, IKZF1,* and *ZNF143,* among others., using the same significance and effect size cutoffs (Fig. 2, E and F, and table S2). Negative regulator TFs for CD19 include *KAT7, ZNF608,* and *BCL11A* (Fig. 2, E and G, and table S2).

Recurrent *PAX5* P80R mutation in ALL leads to the loss of CD58 expression and leukemia sensitivity to blinatumomab

To identify genomic features associated with *CD58* expression in ALL, we examined RNA sequencing (RNA-seq)–based *CD58* transcript quantification in 1988 children and adults with ALL representing 20 molecular subtypes (*31*). There is wide interpatient variability in *CD58* expression, highest in *TCF3-PBX1* ALL and lowest in ALL carrying the *PAX5* P80R mutation (10.75 ± 1.08 versus 7.51 ± 0.68, respectively; Fig. 3A). ALL with *PAX5* P80R mutation universally loses the WT allele by copy number alteration (*31*), representing biallelic loss of *PAX5*. Although *CD19* expression also differs by ALL subtype, it was not related to *PAX5* mutation
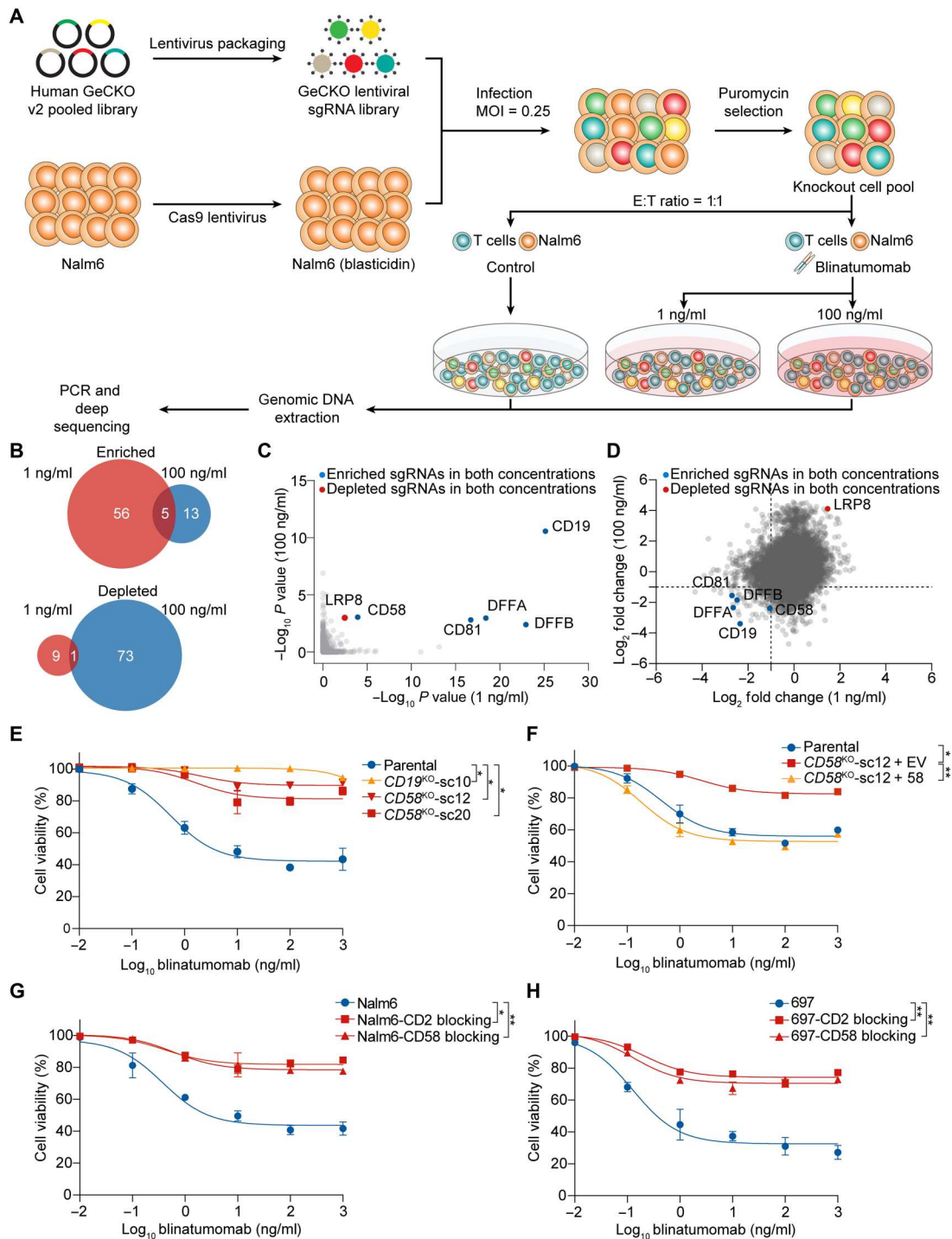
Fig. 1. Genome-wide CRISPR screen identifies B-ALL intrinsic factor governing leukemia sensitivity to blinatumomab in vitro. (**A**) Nalm6-Cas9 cells were transduced with the human Genome-Scale CRISPR Knock-Out (GeCKO) v2 pooled library with six single guide RNAs (sgRNAs) per gene and 1000 nontargeted controls with a multiplicity of infection (MOI) of 0.25. Transduced cells were selected using puromycin, and then incubated with human $CD3^+$ T cells as effector-to-target cell ratio (E:T) = 1:1 with blinatumomab (1 or 100 ng/ml). Cells were collected 7 days after coinoculation, and sgRNAs were amplified for sequencing with NovaSeq. (**B**) The overlap of enriched or depleted sgRNAs after blinatumomab treatment at two different drug concentrations. PCR, polymerase chain reaction. (**C** and **D**) Comparison of CRISPR screen results from two conditions (1 versus 100 ng/ml), plotted by *P* value (C) or $\log_2$ fold change (D). Red and blue dots indicate positive and negative regulators of blinatumomab sensitivity, respectively. Cell survival essential genes were excluded. *LRP8*: LDL Receptor Related Protein 8; *DFFA*: DNA Fragmentation Factor Subunit α; *DFFB*: DNA Fragmentation Factor Subunit β. (**E**) Blinatumomab cytotoxicity on B cell acute lymphoblastic leukemia (B-ALL) cell line Nalm6 was greatly diminished by *CD58* or *CD19* knockout, with T cell coculture for 24 hours. (**F**) Reintroduction of CD58 expression in *CD58*^KO Nalm6 cells restored leukemia sensitivity to blinatumomab in the presence of T cells. EV, empty vector. (**G** and **H**) Anti-CD2 or CD58 antibody (5 μg/ml) markedly blunted B-ALL cell lines [(G) Nalm6 and (H) 697] sensitivity to blinatumomab with T cell coculture for 24 hours. Error bars are SDs of three biological replicates. *P < 0.05; **P < 0.01. Statistical analysis was performed by paired *t* test using Prism GraphPad.
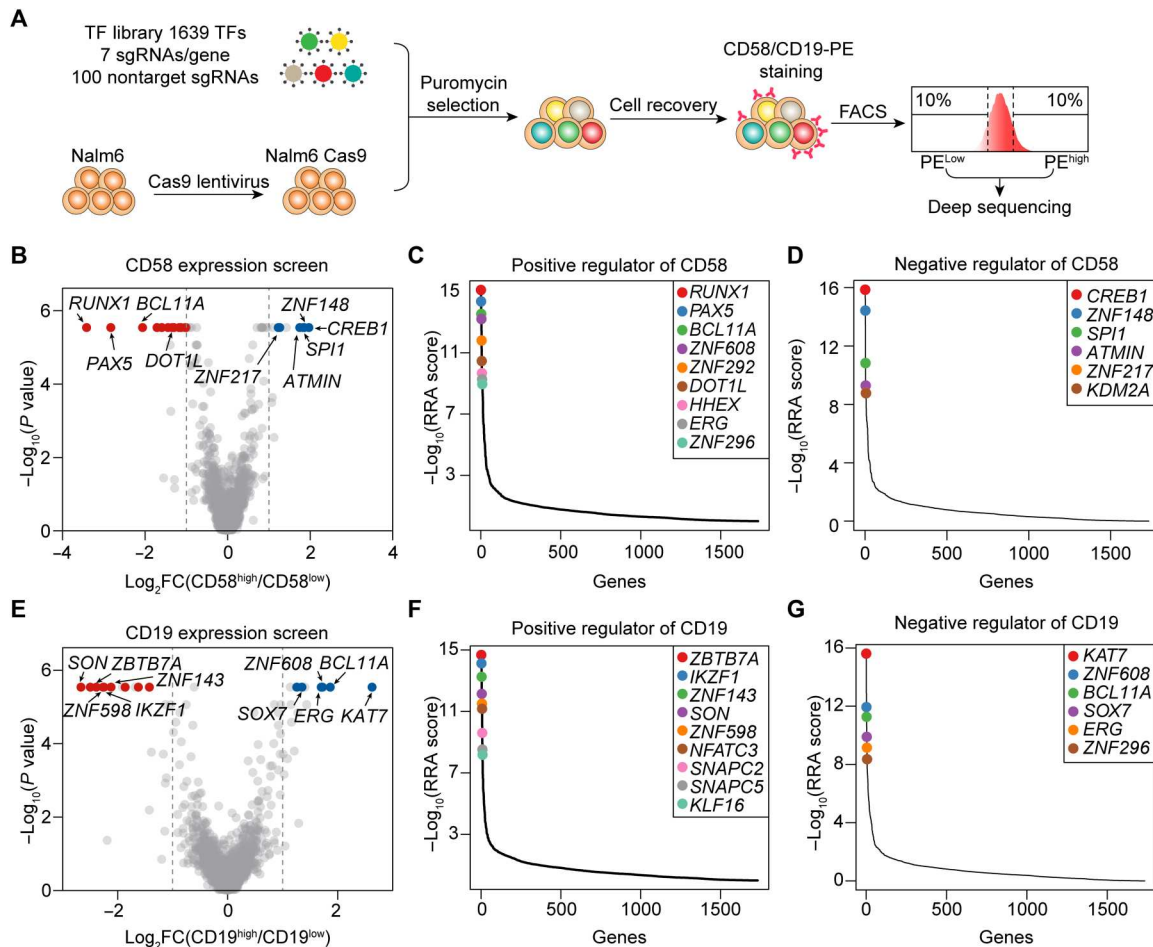
Fig. 2. CRISPR screen of 1639 TF genes identifies positive and negative regulators of CD58 and CD19 expression in B-ALL. (**A**) Nalm6-Cas9 cells were transduced with human TF sgRNA library (1638 TFs targeted at seven sgRNAs per gene plus 100 nontargeted control sgRNAs) with an MOI = 0.25. Transduced cells were selected by puromycin for 7 days. Cells were then stained with anti–CD58-PE or anti–CD19-PE antibodies and sorted for the top 10% and bottom 10% populations based on fluorescence intensity by flow cytometry. sgRNAs were amplified from genomic DNA of each cell population and sequenced with NovaSeq. TF, transcription factor. (**B**) Volcano plot shows genes that positively or negatively regulate CD58 expression [red and blue, respectively, indicating those with $P < 0.05$, $\log_2$ fold change (FC) > 2, and RRA score < 1×10^{-8}]. (**C** and **D**) The positive (C) or negative (D) regulators of CD58 were ranked based on the RRA score. Genes with RRA scores <1×10^{-8} were marked by different colors. (**E**) Volcano plot shows genes that positively or negatively regulate CD19 expression (red and blue, respectively, indicating $P < 0.05$, $\log_2$ fold change > 1, and RRA score < 1×10^{-8}). (**F** and **G**) Positive (F) or negative (G) regulators of CD19 were ranked by the RRA score. Genes with RRA scores <1×10^{-8} were marked by different colors.

(fig. S7). *PAX5* P80R mutation occurs in 2.2% of patients with ALL and is characterized by a distinctive global expression profile as well as the loss of the WT allele, mostly via a focal deletion at this locus (*31*). To directly test the effects of this sequence variation on CD58 expression, we developed three *PAX5* isogenic clones of the B-ALL cell line 697, with WT/WT, WT/frameshift (WT/Fs), and P80R/frameshift (P80R/Fs) genotype, respectively (fig. S8). As shown in Fig. 3 (B and C), cells with biallelic loss of *PAX5* (P80R/Fs) exhibited the lowest CD58 expression by flow cytometry and Western blot, 80% decrease compared to 697 cells with WT *PAX5* (flow cytometry). Cells with hemizygous *PAX5* loss showed intermediate CD58 expression. When treated with blinatumomab, both WT/Fs and P80R/Fs cells were markedly resistant to T cell–mediated lysis, compared to the WT clone of the 697 cell line (Fig. 3D). By contrast, CD19 expression did not change substantially between 697 clones with different *PAX5* genotypes, as determined by RNA-seq and flow

cytometry (fig. S9, A to C). Reintroducing CD58 by ectopic expression reversed the drug resistance phenotype in vitro (Fig. 3, E to G), which further ruled out the influence of CD19 down-regulation in blinatumomab resistance in this context.

To validate the influence of *PAX5* P80R on blinatumomab response in patients, we further tested a panel of ALL xenografts of different subtypes for blinatumomab response in vitro. Patient-derived xenografts (PDXs) of Ph-like *CRLF2*, *ZNF384*, and *PAX5*alt subtypes exhibited similar sensitivity to blinatumomab, whereas the PDX that harbors the *PAX5* P80R mutation has the lowest CD58 expression and was most resistant to this drug (Fig. 3, H to J, and fig. S9, E and F). Ectopic expression of CD58 largely restored the sensitivity of *PAX5* P80R PDX to blinatumomab (fig. S10). Last, besides Nalm6 (*DUX4*) and 697(*TCF3-PBX1*), we also tested three other cell lines of distinctive subtypes with varying levels of CD19 and CD58 expression, namely, REH
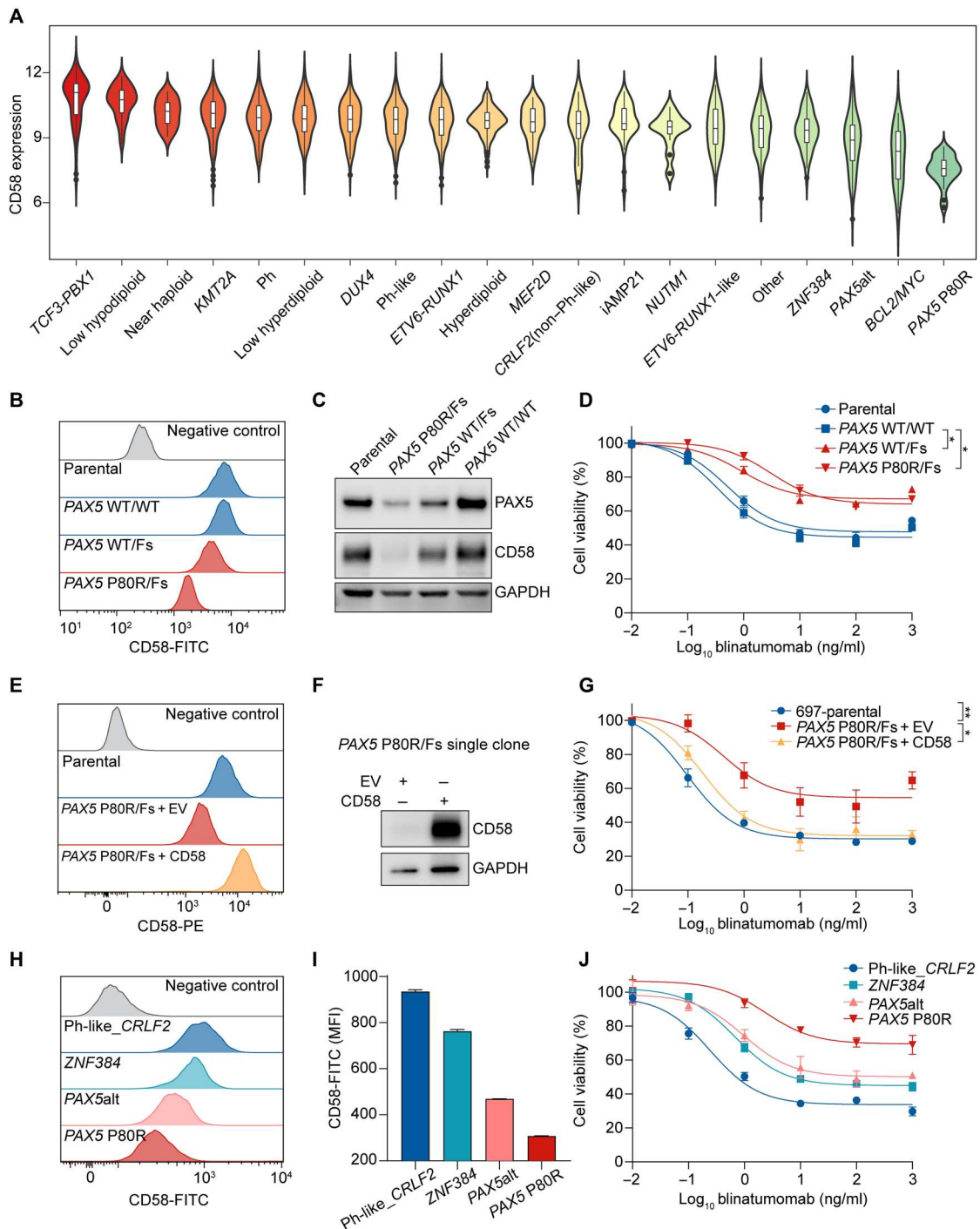
Fig. 3. PAX5 P80R mutation affects B-ALL response to blinatumomab by regulating *CD58* transcription. (**A**) *CD58* expression across 20 molecular subtypes of B-ALL subtypes in 1988 children and adults. (**B** and **C**) CD58 expression in the isogenic B-ALL 697 cell line with different *PAX5* genotypes [wild type/wild type (WT/WT), WT/ frameshifts (WT/Fs), and P80R/frameshifts (P80R/Fs)] and their differential sensitivity to blinatumomab in vitro. CD58 was detected by flow cytometry using CD58-PE fluorescent antibody (B). PAX5 and CD58 expression were also validated by Western blotting, with glyceraldehyde-3-phosphate dehydrogenase (GAPDH) as the loading control (C). (**D**) 697 clones with *PAX5* WT/Fs and *PAX5* P80R/Fs genotype showed significantly diminished sensitivity to blinatumomab with T cell coculture. (**E** to **G**) Reintroduction of CD58 expression in *PAX5* P80R/Fs 697 cells restored sensitivity to blinatumomab. Validation of ectopic expression of CD58 in the *PAX5* P80R/Fs 697 cells by flow cytometry using CD58-PE fluorescent antibody (E) and Western blotting, with GAPDH used as the internal control (F). Blinatumomab cytotoxicity in *PAX5* P80R/Fs 697 cells with versus without CD58 reexpression (G). (**H** to **J**) Blinatumomab cytotoxicity in primary ALL blasts with varying levels of CD58 expression. CD58 expression was quantified by flow cytometry using CD58–fluorescein isothiocyanate (FITC) fluorescent antibody in four cases of ALL with different subtypes (Ph-like_*CRLF2*, *ZNF384*, *PAX5*alt, and *PAX5* P80R) (H and I). Blinatumomab cytotoxicity was lowest in patient-derived xenograft (PDX), which harbors the *PAX5* P80R mutation with the lowest CD58 expression (J). Error bars are SDs of three biological replicates. *$P < 0.05$; **$P < 0.01$. Statistical analysis was performed by paired t test using Prism GraphPad. MFI, mean fluorescence intensity.

(*ETV6-RUNX1*), RS4;11 (*KMT2A*-rearranged), and SUP-B15 (*BCR-ABL1*) (fig. S11A). SUP-B15, which has the lowest CD58 expression, was also most resistant to blinatumomab (fig. S11B). Ectopic expression of CD58 reversed the drug resistance phenotype of SUP-B15 in vitro (fig. S11, C and D).

PAX5-driven enhancer at the *CD58* locus

To delineate the molecular mechanisms underlying the association of *PAX5* mutation with CD58 suppression in ALL, we comprehensively profiled epigenomic marks within this genomic region in 697 cells with WT/Fs, P80R/Fs, and WT/WT genotypes. PAX5 chromatin immunoprecipitation sequencing (ChIP-seq) identified a prominent PAX5 binding site within intron 1 of the *CD58* gene, and PAX5 binding decreased in WT/Fs cells and was completely eliminated in the P80R/Fs clones, suggesting a loss-of-function effect of the P80R mutation (Fig. 4, A and B). This locus was also characterized by H3K27ac and H3K4me3 marks as determined by histone ChIP-seq, signifying its enhancer activity, which was lost in isogenic cells with mutant PAX5 (Fig. 4, A and B). Consistently, Assay for Transposase-Accessible Chromatin sequencing (ATAC)-seq profiling of these samples showed a similar pattern of open chromatin status at this locus that was PAX5 dependent (Fig. 4A). By comparison, PAX5 binding was also observed in the *CD19* promoter region, but P80R mutation had only modest effects on histone modification and chromatin accessibility (fig. S12). To validate the importance of the intronic enhancer in regulating CD58 expression, we performed CRISPR interference experiment in 697 cells (Fig. 4C). As shown in Fig. 4 (C to E), blocking this genomic region by the deactivated CRISPR associated protein 9 (dCas9)-Krüppel associated box (KRAB)-sgRNA complex significantly down-regulated CD58 expression. We further disrupted the two consensus PAX5 motifs within this enhancer using CRISPR editing (Fig. 4F), both of which led to significant down-regulation of CD58 expression measured by flow cytometry (Fig. 4, F and G). Luciferase reporter assay confirms the robust enhancer activity of this genomic fragment [595 base pairs (bp) flanking the PAX5 binding site]; the deletion of either one of the PAX5 motifs resulted in a marked decrease in luciferase activity compared to the WT enhancer (Fig. 4H).

CD58 expression is essential for blinatumomab-induced T cell activation and proliferation in vitro

Because CD58 interacts with CD2 to aid T cell activation, we hypothesize that, in the absence of CD58, B-ALL can no longer trigger T cell activation. T cells incubated with WT Nalm6 cells showed a robust activation as determined by CD69 and CD25 expression, upon exposure to blinatumomab (1 ng/ml) for 2 days. By contrast, T cell cocultured with *CD58*^KO ALL clone showed a substantial decrease in activation (63.6 and 77.1% fold decrease of CD69^+ and CD25^+ T cells), and T cell activation was completely absent with *CD19*^KO Nalm6 cells (Fig. 5, A and D). Blinatumomab itself failed to activate T cells without B-ALL coculture (fig. S13). The lack of T cell activation was consistent in both CD4^+ and CD8^+ subsets (Fig. 5, B, C, E, and F). Last, we also examined T cell proliferation upon exposure to blinatumomab and ALL cells of different genotypes at *CD58* and *CD19*. In the coculture assay, both *CD58*^KO and *CD19*^KO ALL cells failed to induce T cell proliferation by blinatumomab (1 ng/ml), whereas T cells proliferated robustly over 5 days with WT Nalm6 and blinatumomab (Fig. 5G and fig. S14). Therefore, we conclude that leukemia expression of CD58

is essential for blinatumomab-induced T cell immune response against B-ALL. Consistent with this, the *PAX5* P80R/Fs 697 cells, which have significantly lower levels of CD58 (Fig. 3C), have similar defects in T cell activation (fig. S15, A to F) and proliferation (fig. S15, G to J) compared to parental 697 cells.

To further elucidate the function of CD58 on T cell immune response toward B-ALL, we performed RNA-seq and ATAC-seq of T cells cocultured with parental, *CD58*^KO, or *CD19*^KO Nalm6 cells. Principal components analysis (PCA) of RNA-seq data showed that blinatumomab treatment drastically reprogrammed T cell gene expression profile in the presence of either parental or *CD58*^KO B-ALL cells, although with a substantial divergence between the two groups (Fig. 5H, red versus blue squares). The loss of CD19 in B-ALL (*CD19*^KO Nalm6) eliminated its interaction with T cells that consequently did not exhibit a substantial change in expression by blinatumomab (Fig. 5H, orange circles versus squares). Comparing T cells cocultured with parental versus *CD58*^KO Nalm6 cells, we identified 111 genes that were uniquely up-regulated by blinatumomab in the former (Fig. 5I and tables S3 and S4), and these genes were not differentially expressed without the bispecific antibody (Fig. 5J). Gene ontology analysis of these 111 genes indicated an enrichment of tricarboxylic acid cycle, mitochondrial membrane, and oxidative phosphorylation (e.g., *MT-CYB*, *MT-ND4*, *MT-ND5*, and *MT-ATP6*; fig. S16) and in immune response and cytokine signaling pathways (e.g., *IL2RA*, *GZMA*, *IFNG*, and *GZMB*; fig. S16). Results from ATAC-seq of T cells largely confirmed the RNA-seq–based findings. For example, ATAC-seq signal in the *IFNG* promoter region was notably lower in T cells cocultured with *CD58*^KO Nalm6, compared to those with parental Nalm6 (Fig. 5K). We also directly quantified interferon-γ (IFN-γ) level in the T cell–Nalm6 coculture, which was 13.88-fold higher in the parent Nalm6 group (Fig. 5L). Analyzing single-cell RNA-seq (scRNA-seq) data of blinatumomab-stimulated T cells (*3*), we observed a much more profound transcriptomic response on the single-cell level in T cells cocultured with ALL cells with high CD58 expression (RS4;11) compared to that seen with ALL cells with low CD58 expression (SUP-B15) (fig. S17). Collectively, these data indicate that the loss of CD58 reduced T cell activation.

DISCUSSION

Despite the marked activity of blinatumomab in B-ALL, drug resistance occurs frequently, and the underlying mechanisms, especially in those cases that retain CD19 expression, are unclear. In this study, we performed a genome-wide CRISPR-Cas9 knockout screen to comprehensively identify leukemia intrinsic factors involved in blinatumomab response. Focusing on one of the top hits, *CD58*, we conducted a series of in vitro experiments using B-ALL cell lines and PDX samples. Then, we systematically screened 1639 TF genes for regulators of CD58 and CD19 expression in B-ALL. Further analysis showed that *CD58* expression in ALL with the *PAX5* P80R mutation was particularly low compared to other molecular subtypes. PAX5 regulated the expression of CD58 by modulating an intronic enhancer within this gene. Furthermore, we showed that CD58 was essential for blinatumomab-induced T cell activation and proliferation in vitro. These findings established the role of CD58 in the blinatumomab-induced immune response of effector T cells and suggested the possibility of individualizing blinatumomab therapy based on genomic findings in ALL cells.

Fig. 4. PAX5-driven enhancer activation at the *CD58* locus. (**A**) PAX5 binding [chromatin immunoprecipitation sequencing (ChIP-seq)], histone modification (ChIP-seq), and open chromatin status (ATAC-seq) at the *CD58* locus in 697 cells with different PAX5 genotypes. ChIP-seq and ATAC-seq signals of PAX5-edited 697 clones in *CD58* gene locus. The blue line marks the PAX5-driven intronic enhancer. (**B**) ChIP–quantitative PCR (qPCR) validation of PAX5 binding and histone modification at the *CD58* enhancer. Cell lysates were subjected to pull-down using respective antibodies, and the enhancer region DNA was quantified by qPCR (primers indicated by the red line). Fold change in the binding of PAX5, H3K27ac, and H3K4me3 on enhancer regions was determined by comparing them to unenriched total input samples (Enhancer). Primer targeting ~50-kb upstream of *CD58* transcription start site (TSS) was used as negative control (Negative). (**C**) The influence of the *CD58* intronic enhancer region on CD58 expression was validated by CRISPRi assay. Six sgRNAs localized across the *CD58* intronic enhancer region were transfected into 697 cells that constitutively express dCas9-KRAB. (**D** and **E**) CD58 expression was measured by flow cytometry using CD58-FITC antibody in sgRNA-transfected (sgRNA1 + 2, sgRNA3 + 4, and sgRNA5 + 6) or untransfected (697-dCas9-KRAB) cells. (**F**) The influence of PAX5 binding at the intronic enhancer on CD58 expression was validated using CRISPR editing. Two sgRNAs localized on each PAX5 motif were transfected into 697 cells that constitutively express Cas9. (**G**) CD58 expression was measured using flow cytometry in sgRNA-transfected or untransfected cells. (**H**) The enhancer activity of the genomic sequence encompassing the PAX5 binding sites at this locus was quantified using luciferase assay. PAX5 motif was deleted in the same construct to determine the importance of PAX5 binding in enhancer activity. Error bars are SDs of three biological replicates. ***$P < 0.001$. Statistical analysis was performed by Student's *t* test using Prism GraphPad.
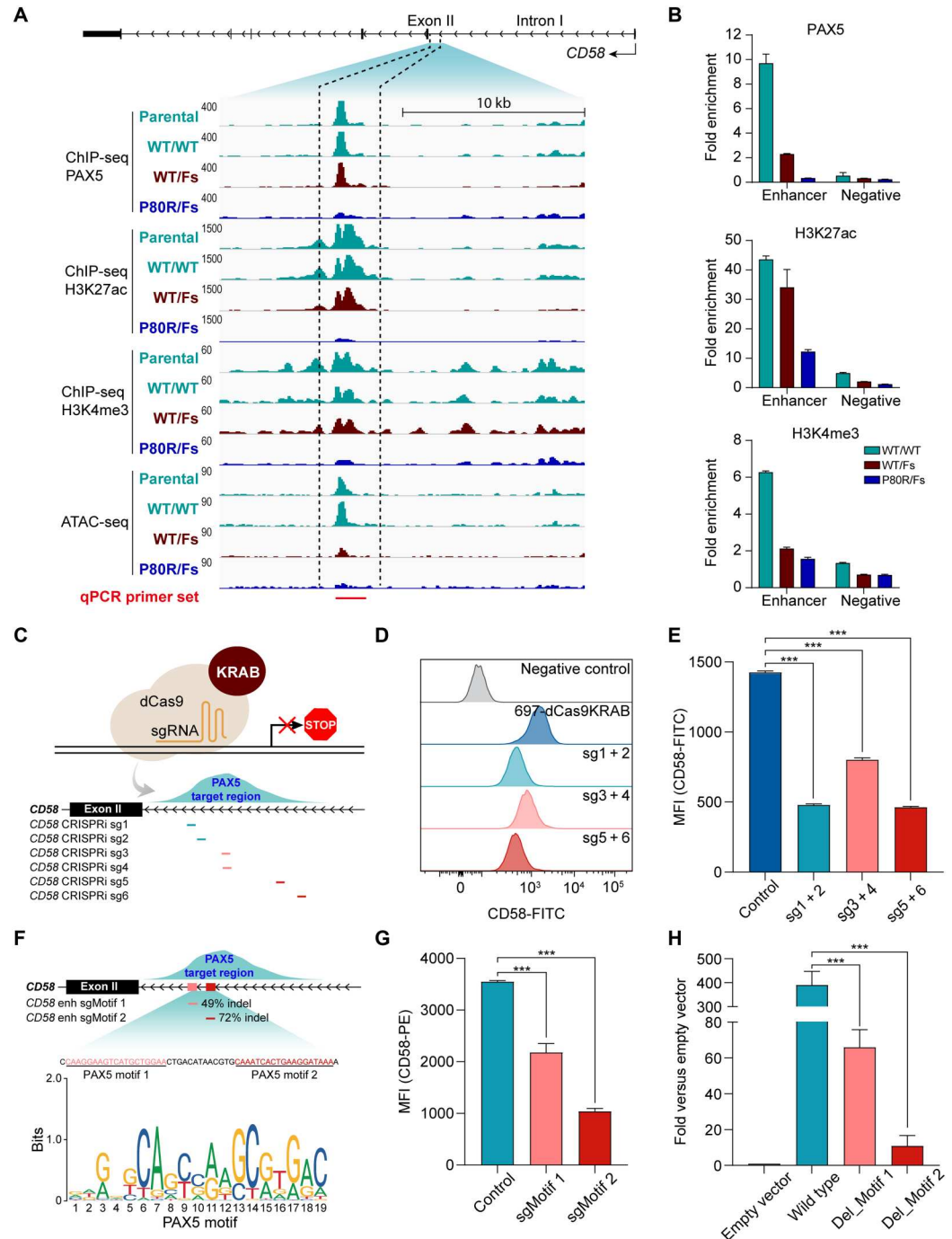
Although the work presented here largely focused on CD58, the mechanism of blinatumomab resistance is undoubtedly multifactorial and likely to involve other genes (*32*). For example, our CRISPR screen at blinatumomab (100 ng/ml) yielded a relatively smaller number of hits because of the small number of cells that survived this level of cytotoxic pressure. Therefore, we reason that genes identified in these conditions are likely to have strong effects on

drug resistance, and hits of moderate impact were possibly missed by this approach.

CD58 is a cell adhesion molecule expressed on antigen-presenting cells (*33*). As the ligand of CD2 on T cells, CD58 strengthens the adhesion between T cells and antigen-presenting cells. The interaction of CD2 and CD58 is important in providing the costimulatory signal for T cell activation, proliferation, and cytokine production (*29*, *34*, *35*). *CD58* mutations have been identified and linked to

Fig. 5. *CD58* depletion in B-ALL abolishes T cell activation and proliferation despite blinatumomab treatment. (**A** to **F**) T cell activation was measured as % CD69 positivity by flow cytometry within all T cells (A), CD4+ (B), and CD8+ (C) T cells. (**D** to **F**) Similarly, CD25 positivity was measured as another marker of T cell activation in each of these three populations. B-ALL cells were incubated with blinatumomab and T cells for 2 days. Data are presented as means ± SEM. (**G**) Carboxyfluorescein diacetate succinimidyl ester (CFSE) staining shows the proliferation of T cells after 3 and 5 days of coculture with Nalm6 and blinatumomab (1 ng/ml) with different phenotypes. Cells with lower CFSE signals represent those proliferated upon blinatumomab treatment. (**H**) Principal components analysis (PCA) of RNA sequencing (RNA-seq) of T cells cocultured with parental (blue), *CD58*KO (red), or *CD19*KO (orange) Nalm6, with (square) or without (circle) blinatumomab. (**I** and **J**) Differential gene expression in T cells cultured parental or *CD58*KO Nalm6 cells after blinatumomab treatment (I) or exposed to vehicle control (J). TPM, transcripts per million. (**K**) Open chromatin status (ATAC-seq) and exon expression (RNA-seq) at the *IFNG* gene locus in T cells cocultured with parental (blue) or *CD58*KO (red) Nalm6 in the presence of blinatumomab. Each row represents an independent experiment. (**L**) T cell secreted significantly higher levels of interferon-γ (IFN-γ) when cocultured with parental Nalm6 than with *CD58*KO Nalm6, in the presence of blinatumomab. Error bars are SDs of three biological replicates. **P <0.001; ***P < 0.0001. Statistical analysis was performed by Student's *t* test using Prism GraphPad.
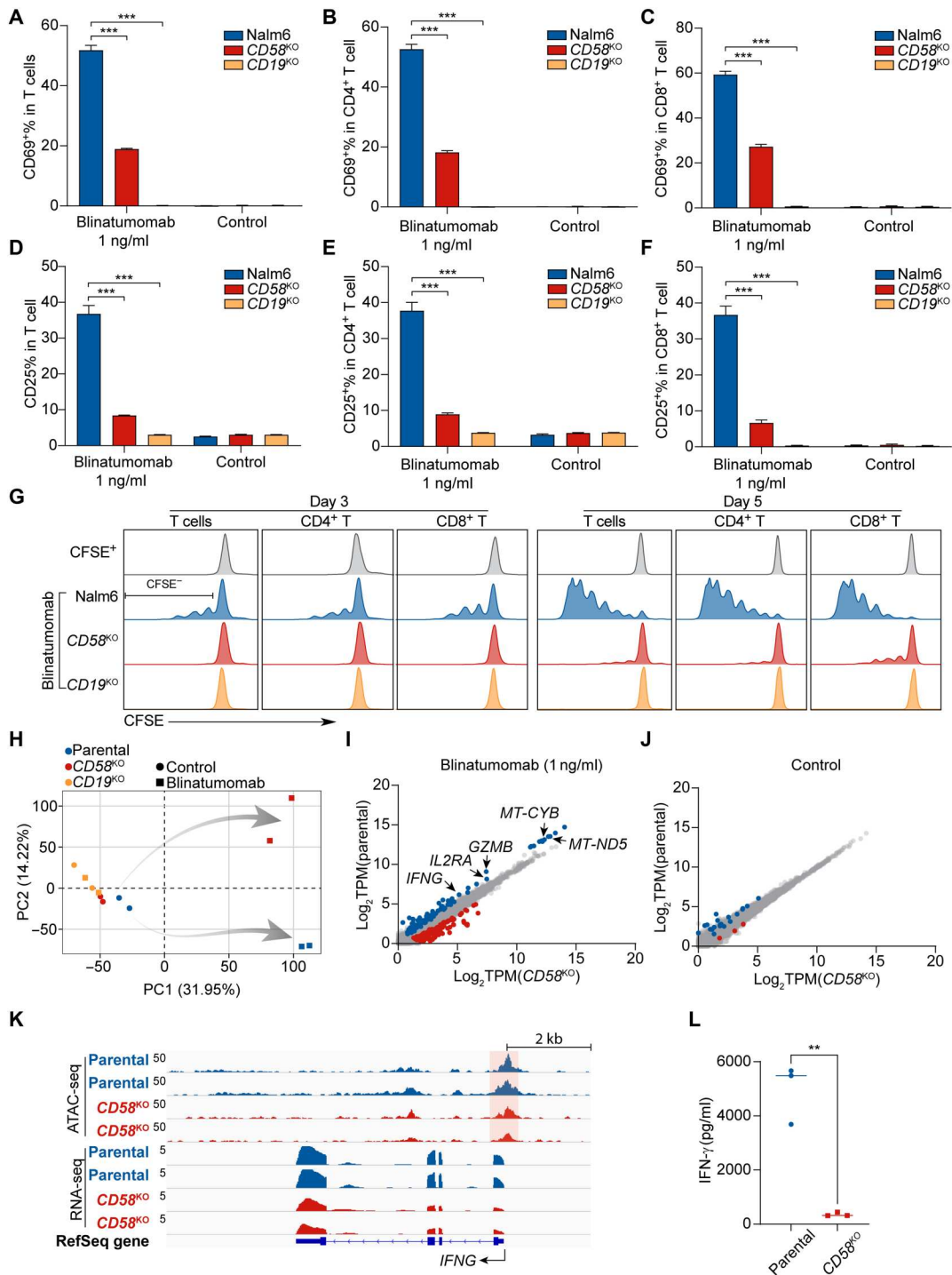
immune resistance of B lymphocyte malignancies, including diffuse large B cell lymphoma and Hodgkin lymphoma (*29*, *34*, *35*). This is in line with the profound effects of CD58 on blinatumomab sensitivity in B-ALL, as documented in our study. Recently, evidences have also emerged that suggest the role of CD58 in activating chimeric antigen receptor (CAR) T cells targeting CD19+ B-ALL; the knockout of *CD58* in B-ALL cells decreased the response to CD19 CAR T cells (*36*). *CD58* loss is associated with the inferior outcome

of CD19 CAR T cell therapy (*37*). Analyzing recently published scRNA-seq data of blinatumomab-stimulated T cells, we observed that high CD58 expression ALL cells showed a much more profound transcriptomic response on the single-cell level when cocultured with T cells compared to that seen with ALL cells with low CD58 expression (fig. S17) (*3*). Together, these findings provide previously unknown insights into the role of CD58-mediated

costimulatory signals in T cell activation and therefore immunotherapy efficacy.

B-ALL consisted of more than 20 molecular groups, characterized by multiple inherited and somatic genetic alterations, including chromosomal rearrangements, mutations, and heterogeneous genomic alterations (*38*, *39*). *CD58* low expression was particularly notable in cases with *PAX5* P80R mutation, and *CD58* was one of the top differentially expressed genes defining this subtype. By contrast, there was substantial heterogeneity in *CD58* expression in ALL with other types of *PAX5* alterations, e.g., focal deletion or translocation involving *PAX5*. Because ALL with *PAX5* P80R mutation universally loses the WT allele by copy number alteration, this may explain the marked down-regulation of *CD58* in this subtype. In addition, low *CD58* expression was also seen in other ALL subtypes (Fig. 3A), albeit less frequent, suggesting PAX5-independent mechanisms of CD58 regulation, which are yet to be identified. PAX5 is a known transcriptional regulator of CD19 expression (*32*, *40*), which was also confirmed in our TF screen for CD19, although it was not one of the top hits as seen with the CD58 screen (table S2). It is likely that PAX5 modulates both CD19 and CD58 in B cells, but the exact impact may vary depending on cellular context (e.g., B-ALL subtype). It is important to point out that the effect of PAX5 P80R is highly specific to CD58, as validated by RNA-seq or flow cytometry of isogenic 697 cells (fig. S9, A to C), as well as in 1988 patients with ALL (fig. S7). We reason that *PAX5* P80R functions differently from simple *PAX5* deletion and therefore may have a selective effect on enhancer activity at the *CD58* locus with minimal impact on CD19. Linking ALL genomic lesions to blinatumomab efficacy is of potential clinical relevance, because it would enable individualized therapy. For example, *PAX5* P80R–positive patients with ALL are unlikely to respond, but the patients would still experience treatment-related toxicity. Avoidance of blinatumomab for these patients would increase the precision and reduces treatment cost. The same argument can be made for other ALL cases with low CD58 expression, raising the question whether CD58 should be included in the diagnostic panel of ALL to direct the selection of patients for blinatumomab therapy. A recent study compared leukemia genomics in a cohort of 44 adult patients with B-ALL with or without response to blinatumomab (*23*) but did not observe an association of *CD58* expression with response after accounting for CD19. Careful examination of the dataset indicates that nearly all cases included this study had a relatively high level of *CD58*, with the lowest expression being ~2-fold higher than the median value in ALL with *PAX5* P80R. Therefore, we hypothesize the following: (i) The mechanism of blinatumomab is heterogeneous; the loss of *CD58* might only explain a fraction of the cases and may not show overall statistical significance with a relatively small sample size. (ii) There is a minimal threshold of CD58 in B-ALL for blinatumomab response, above which further up-regulation of CD58 expression no longer increases leukemia response to this drug. That said, future studies are warranted to validate the impact of CD58 on blinatumomab efficacy in vivo and also to define the exact level of CD58 expression in B-ALL that is required to trigger T cell activation by blinatumomab. (iii) *CD58* expression at the RNA level does not represent the amount of functional CD58 on the leukemia cell surface. Flow cytometry or Cytometry by time-of-flight (CyTOF) assays might be more informative in evaluating the effects of CD58 on blinatumomab response, and this needs to be considered in future studies.

Bispecific antibodies have garnered increasing interest in the cancer immunotherapy space, with a number of agents entering clinical trials besides blinatumomab (*41*, *42*). For example, mosunetuzumab, a CD3-CD20 bispecific antibody, showed a high response rate in patients with B cell lymphoma either as a single agent or when in combination with the CHOP regimen, which is a chemotherapy combination that includes cyclophosphamide, doxorubicin, vincristine, and prednisolone (*43*, *44*). In phase 1 trials, odronextamab and glofitamab induced durable complete responses in patients with highly refractory B cell non-Hodgkin lymphoma, including those refractory to CAR T therapy (*45*, *46*). Bispecific antibodies targeting other B cell surface markers have also been developed, e.g., JNJ-75348780, a bispecific antibody targeting CD3 and CD22 (*47*). The influence of CD58 on the bispecific antibody efficacy was recently described for solid tumors and lymphoma (*48*). It is possible that CD58 is required for the efficacy of this entire class of agents because of its essential role in mediating T cell–tumor engagement. With the normal expression of the target cell surface marker, triggering CD58 expression might be a feasible way to increase the treatment effect of these antibody drugs.

In summary, we systematically identified genetic determinants of blinatumomab sensitivity in B-ALL, integrating genome-wide CRISPR screens and leukemia genomic profiling. Our results provide previously unknown insights into the mechanisms of acquired drug resistance and point to opportunities for genomics-guided individualization of blinatumomab therapy in ALL.

MATERIALS AND METHODS

Human leukemic cell lines and PDX

Nalm6 (CRL-3283), REH (CRL-8286), SUP-B15 (CRL-1929), and RS4;11 (CRL-1873) cell lines were purchased from the American Type Culture Collection, and the 697 (ACC42) cell line was purchased from Deutsche Sammlung von Mikroorganismen und Zellkulturen . All the cell lines used in this study were cultured in RPMI 1640 (Gibco, 11875093) with fetal bovine serum (FBS; HyClone, SH30071.03). Human telomerase reverse transcriptase (hTERT) transduced MSCs (mesenchymal stem cells) were maintained in RPMI 1640 (Gibco, 11875093) with 2 mM L-glutamine (Gibco, 25030081), 20% FBS (GE Life Sciences, SH30071.03), and 1 μM hydrocortisone (Sigma-Aldrich, H0396). PDX samples were generated as described previously (*49*) by injecting primariy patient samples in to 8-week-old female NOD.Cg-*Prkdc*^{scid} *Il2rg*^{tm1Wjl}/SzJ (NSG) mice. *CD58* and *CD19* knockout single clones were generated in Nalm6 cells transduced with Cas9 and sgRNAs targeting *CD58* or *CD19*. *PAX5* P80R knock-in clones were generated in 697 cells using CRISPR-mediated homology-directed repair (HDR). Details of sgRNA, genotyping primers, and HDR template can be found in table S5.

Genome-wide CRISPR-Cas9 knockout library screen

The human Genome-Scale CRISPR Knock-Out (GeCKOv2A) CRISPR knockout library was purchased from Addgene (1000000048) (*50*). The Cas9-expressing Nalm6 cells were a gift from W. E. Evans (*51*). We transduced Nalm6 Cas9 cells with either GeCKOv2A Lib A or B by spin infection. Briefly, cells were seeded in 12-well plates at a concentration of 1.5 million cells per ml, 2 ml for each well, and lentivirus was added into each well at an MOI at 0.25. The cell virus mixture was spinning at 2000 rpm

at 30°C for 2 hours. After 2 days of infection, cells were selected with puromycin (5 µg/ml) for 5 days. After that, human Pan−T cells (STEMCELL Technologies, 70024) were mixed with Nalm6 cells at an effector-to-target cell ratio (E:T) of 1:1. Cell mixtures were treated without or with blinatumomab at 1 or 100 ng/ml and harvested after 7 days. DNA was extracted using the QIAamp DNA Blood Maxi Kit (QIAGEN, 51192). The sgRNA region was polymerase chain reaction (PCR)–amplified and sequenced via Illumina HiSeq 2500 (50, 52).

In vitro blinatumomab sensitivity test

Blinatumomab was provided by Amgen Inc. under a research collaborative agreement. Leukemia cell lines or PDX samples were stained with PKH26 (Sigma-Aldrich, PKH26GL-1KT) and then mixed with human peripheral blood Pan−T cells (STEMCELL Technologies) at E:T ratio = 1:1 (36,000 cells in 80 µl per well for each cell types). Blinatumomab was added at 1000, 100, 10, 1, 0.1, and 0.01 ng/ml (40 µl per well). Viability in PKH26$^+$ cells was detected by flow cytometry using 4′,6-diamidino-2-phenylindole staining at 24 hours. Cell viability in each dosage was calculated by dividing the live cell population in each dosage by the live cell population in the control group without blinatumomab treatment. For CD2 or CD58 blocking experiments, CD2 (BioLegend, 309202) or CD58 (BioLegend, 330902) antibodies were added into the culture media at a final concentration of 5 µg/ml.

TF library CRISPR-Cas9 screen

The human TF CRISPR knockout pooled library, which contains 1639 TFs and seven sgRNAs per gene, was a gift from C. Li (30). The infection method was the same as described above. Infected cells were selected by puromycin and stained with phycoerythrin (PE) anti-human CD19 (BioLegend, clone SJ25C1) or PE mouse anti-human CD58 (BD Biosciences, clone L306.4) antibodies and sorted for PE^{high} and PE^{low} populations after 7 days. Three independent replicates were performed. The sgRNA sequences were recovered by genomic PCR and detected by Illumina sequencing (30). Sequencing was performed on a NovaSeq 6000 (Illumina). Sequence data were analyzed using MAGeCK (version 0.5.9.5) (53). The differentially enriched sgRNAs were defined by comparing cells in the top 10% versus bottom 10% of CD58-PE or CD19-PE populations.

Ethical approval for research

Human subject research was approved by institutional review boards at St. Jude Children's Research Hospital, and informed consent was obtained from parents, guardians, or patients, and assent from patients, as appropriate. All animal experiments were conducted according to the protocol (protocol number: 624) approved by the St. Jude Institutional Animal Care and Use Committee.

Lentivirus production and transduction

Cl20-EF1α−green fluorescent protein (GFP) plasmid backbone was generated by St. Jude Vector core and used to create cl20-(Elongation factor 1 α) EF1α-internal ribosome entry site (IRES)-GFP lentivirus backbone used in this study. EF1α and IRES-GFP sequences were PCR-amplified from cl20-EF1α-GFP and cl20c-MSCV-IRES-GFP (generated by St. Jude Vector core) and cloned into Kpn I− and Age I−digested cl20-EF1α-GFP by using NEBuilder HiFi DNA

Assembly Master Mix (NEB, E5520). Then, human *CD58* cDNA was synthesized and cloned into the Eco RI−digested cl20-EF1α-IRES-GFP backbone by using NEBuilder HiFi DNA Assembly Master Mix. Primers for plasmid construction can be found in the supplementary tables.

Lenti-X 293 cells (Clontech) were cultured in Dulbecco's modified Eagle's medium with high glucose (4.5 g/liter) (Gibco, D6429) containing 10% FBS at 37°C with 5% CO$_2$. Lentivirus generation was performed as described previously (54). B-ALL cell lines, including parental and CRISPR knockout/knock-in single clones of Nalm6 and 697, were infected with cl20-EF1α-IRES-GFP (empty vector, EV) or cl20-EF1α-*CD58*-IRES-GFP (CD58) in 12-well plates by adding 10 µl of 100-fold concentrated lentivirus to each well that contains 1 million cells in 1 ml of medium for 48 hours. The GFP$^+$ cells were sorted by flow cytometry and used for in vitro drug treatment experiments. The *PAX5* P80R PDX sample was infected with EV or CD58 lentivirus as described above. After 12 hours of infection, cells were collected and injected into NSG mice. After engraftment, the GFP$^+$ population from the spleen were isolated by flow cytometry, mixed with GFP$^-$ splenic population (to reach 2 million cells total), and then injected into NSG mice again. After three rounds of engraftment, GFP$^+$ population for both EV and CD58 groups reached ~50% in splenic blast and were sorted and plated on an MSC-coated plate for ex vivo blinatumomab sensitivity test, same as B-ALL cell lines.

Flow cytometry and Western blot antibodies

PE anti-human CD19 antibody (BioLegend, clone SJ25C1), Percpcy5.5 anti-human CD19 antibody (Thermo Fisher Scientific, clone HIB19), PE mouse anti-human CD58 antibody (BD Biosciences, clone L306.4), and fluorescein isothiocyanate (FITC) mouse anti-human CD58 antibody (BD Biosciences, clone 1C3) were used for CD19 or CD58 expression analysis for leukemia cell lines. Western blot was performed using the following antibodies: anti-PAX5 antibody (Abcam, ab15164), recombinant anti-CD19 antibody (Abcam, ab134114), and anti-CD58 antibody (Abcam, ab196648).

RNA sequencing

Total RNA was purified from 697 (including *PAX5* WT/WT, *PAX5* P80R/Fs, and *PAX5* WT/Fs) and human Pan−T cells that were incubated with leukemia cells with or without blinatumomab treatment by using QIAGEN RNeasy Mini Kit (QIAGEN, 74104). Total RNA library was constructed using an Illumina TrueSeq stranded mRNA library prep kit and sequenced using the NovaSeq 6000 platform (2 × 100-bp paired-end reads). Gene expression was aligned by STAR (version 2.6.0b) (55) under default parameters with the human genome (GRCh37/hg19) and annotation file (GENCODE v19) (56, 57). Differential expression analysis was performed by the edgeR package (58–60). PCA was performed using the built-in R function "prcomp" on all protein-coding genes, and the plot was generated by ggplot.

T cell proliferation analysis

Pan−T cells were stained with CellTrace carboxyfluorescein diacetate succinimidyl ester (CFSE) (Thermo Fisher Scientific, C34554) as described previously (61). Briefly, 7 × 10^6 cells were resuspended using 500 µl of phosphate-buffered saline (PBS) (containing 5% FBS). One microliter of 5 mM CFSE was added into another 500

μl of PBS (contains 5%FBS) at a final concentration of 10 μM. Then, 500 μl of CFSE diluent was added into 500 μl of cell suspension and mixed immediately and incubated at room temperature for 5 min. After washing with 10-fold volume of PBS (which contains 5% FBS) twice, T cells were resuspended in RPMI 1640 (which contains 10% FBS). T cell and leukemia cells were mixed at E:T ratio = 1:1 with or without blinatumomab (1 ng/ml) treatment. Flow cytometry was then performed to detect CFSE signals in T cell population after 3 and 5 days of coculture.

T cell function analysis
Nalm6 cells, including parental, $CD58^{KO}$-sc12, and $CD19^{KO}$-sc10, were incubated with human Pan–T cells (STEMCELL Technologies) at E:T ratio = 1:1 with or without blinatumomab (1 ng/ml) treatment for 2 days. T cells were then isolated by flow cytometry and subsequently used for RNA-seq and ATAC-seq.

ChIP-seq and quantitative PCR
ChIP was performed on 697 parental, 697-$PAX5$ P80R/Fs, 697-$PAX5$ WT/Fs, and 697-$PAX5$ WT/WT using ChIP-IT High Sensitivity Kit (Active Motif, 53040) according to the manufacturer's protocol. A total of 2×10^6 cells were fixed with complete cell fixation solution for 15 min and then stopped by stop solution for 5 min, followed by sonication. Both buffers were provided by the ChIP-IT High Sensitivity kit. The following antibodies were used for ChIP assays: anti-PAX5 (Abcam, ab15164), anti-H3K27Ac [Cell Signaling Technology (CST), 8173S], and anti-H3K4me3 (CST, 9751). Normal rabbit immunoglobulin G (CST, 2729) was used for control ChIP. Primers for ChIP-qPCR analysis are shown in table S5.

ATAC-seq
697 cells (including parental, $PAX5$ WT/WT, $PAX5$ P80R/Fs, and $PAX5$ WT/Fs single clones) and human Pan–T cells that were incubated with leukemia cells with or without blinatumomab treatment were used for ATAC-seq as described before (62). Briefly, cells were counted and diluted into 1 million per 1 ml of fresh media. Ten microliters (containing 10,000 cells) was aliquoted into a 1.5-ml Eppendorf tube and cells were spun at $500g$ for 5 min at 4°C. Transposition mix was made in the following order: (i) 22 μl of nuclease-free water, (ii) 25 μl of 2× Tagment DNA (TD) buffer, (iii) 2.5 μl of Tagment DNA Enzyme (TDE1) transposase, and (iv) 0.5 μl of 1% digitonin (added right before removing supernatant from cell pellets). Supernatant was removed and 2 μl of media was left to ensure the cell pellets were not disturbed. Then, 50 μl of transposition mix was added to cells and mixed gently, and the reaction was incubated at 37°C on a thermomixer at 300 rpm for 30 min. DNA was purified by using the MinElute Reaction Cleanup kit (QIAGEN, 28204), eluted with 10 μl of elution buffer, and amplified for five cycles by adding the following mix: 10 μl of transposed DNA, 2.2 μl of nuclease-free water, 6.25 μl of 10 μM barcoded Nextera primer-F, 6.25 μl of 10 μM barcoded Nextera primer-R, 0.3 μl of 100× SYBR™ Green I Nucleic Acid Gel Stain (Invitrogen, S-7563), and 25 μl of NEBNext High-Fidelity 2× PCR Master Mix (NEB, M0541). PCR cycle was as follows: 72°C for 5 min; 98°C for 30 s; five repeats of 98°C for 10 s, 63°C for 30 s, and 72°C for 1 min, held at 4°C. Then, a quantitative PCR reaction was performed on an Applied Biosystems Real-Time PCR machine using 5 μl of PCR product to determine the additional number of PCR cycles required, which was determined by the cycle that corresponds to one-fourth of the maximum fluorescent intensity. PCR products were subsequently reamplified for six additional PCR cycles, and the product was purified using SPRIselect beads (Beckman Coulter, B23317).

CRISPR interference and CRISPR editing of PAX5 binding sites within the $CD58$ enhancer
CRISPR interference
697 cells with stable expression of dCas9-KRAB were established using lenti-dCas9-KRAB-last plasmid (Addgene, no. 89567). Six sgRNAs targeting the $CD58$ intronic enhancer region were designed and cloned into lentiGuide-Puro (Addgene, no. 52963) plasmid. 697-dCas9-KRAB cells were transduced with sgRNA lentivirus separately (sg1 + 2, sg3 + 4, and sg5 + 6) for 2 days and selected with puromycin (5 μg/ml) for 5 days.
CRISPR editing of PAX5 binding sites
PAX5 motif in PAX5 target region was scanned using the JASPAR 2022 database (https://jaspar2022.genereg.net/). Two consensus PAX5 motifs (MA0014.2 and MA0014.3) identified in *Homo sapiens* were used for scanning using default settings of the website. 697 cells with stable expression of Cas9 were established using lentiCas9-Blast plasmid (Addgene, no. 52962). Two sgRNAs targeting each PAX5 motif were designed and cloned into lentiGuide-Puro (Addgene, no. 52963) plasmid. 697-Cas9 cells were transduced with sgRNA lentivirus separately for 2 days and selected with puromycin (5 μg/ml) for 5 days.

CD58 expressions were determined by flow cytometry. All the high-titer lentivirus was generated with Lenti-X cells (Takara, no. 632180).

Luciferase reporter assay
$CD58$ intronic enhancer region (hg38 chr1:116544766-116545360) was cloned into the Kpn I– and Hind III–digested pGL4.23-miniP backbone plasmid (Promega, E841A) by NEBuilder HiFi DNA Assembly Master Mix (NEB, E5520). PAX5 motif deletion was performed using QuikChange II Site-Directed Mutagenesis Kit (Agilent, 200523). We transiently transfected 697 cells with $CD58$ enhancer–driven reporter plasmid (either WT or with PAX5 motif deletion) and SV40 promoter–driven reporter plasmid using Cell Line Nucleofector Kit R (Lonza, VCA-1001). Luciferase activity was measured after 20 hours of transfection. Primers for plasmid cloning are shown in table S5.

Data access
ChIP-seq, ATAC-seq, and RNA-seq data were submitted to Gene Expression Omnibus (GSE202083).

Analysis of scRNA-seq data
Alignment, barcode assignment, and unique molecular identifier counting
The single-cell RNA-seq datasets generated during the previous study are available in the Sequence Read Archive repository (accession numbers: SRR13518691, SRR13518692, SRR13518693, SRR13518694, SRR13518695, SRR13518696, SRR13518701, and SRR13518702 in BioProject, PRJNA694543) (3). The Cell Ranger 3.1.0 Single Cell software suite (10x Genomics) was implemented to process raw sequencing data. This pipeline performed demultiplexing, alignment (GRCh38), and barcode processing to generate

gene-cell matrices used for downstream analysis. Specifically, data from cell line samples were combined into one dataset for consistent filtering. The initial Seurat object was generated by selecting cells with at least 200 genes detected and genes detected in at least three cells. Only cells with a mitochondria content of less than 10% and a hemoglobin content of less than 25% were kept for further analyses. We normalized the expression level of each gene to 1,000,000 Unique Molecular Identifier (UMIs) per cell and $\log_2$-transformed.

Clustering analysis and data visualization
To classify the cells, the R package Seurat was used (63). The highly variable genes were identified from these cells using Seurat with the default setting. Then, these highly variable genes were used for PCA. For visualization of clustering results, we used t-distributed stochastic neighbor embedding with the first 20 dimensions as the input. Seven immune cell types across all profiled single cells have been identified on the basis of cell type marker genes.

NetBID analysis and driver identification from scRNA-seq data
We adapted the NetBID (data-driven network-based Bayesian inference of drivers) algorithm (64), which was originally designed to identify drivers from bulk omics data to scRNA-seq data to identify immune cell type–specific drivers in remission and relapse mice upon dasatinib treatment. First, we reverse-engineered the transcription and signaling interactomes specific to activated CD4+ T (2012 cells) and activated CD8+ T (225 cells) from their scRNA-seq profiles and B-ALL (1985 patients) from bulk RNA-seq profiles (31) by using the SJARACNe (65) algorithm, an information theory–based algorithm for regulatory network inference. The parameters of SJARACNe were configured as follows: p_value_bootstrap = 1×10^{-7}, p_value_consensus = 1×10^{-5}, and bootstrap_num = 100. On the basis of Gene Ontology classification, we compiled a list of TF genes and signaling molecule genes (N = 1729 and 8863, respectively). TF network and signaling molecule network were generated separately using SJARACNe, with drivers (hubs) linked to their targets through interactions (edges) based on gene-gene relationship derived from their expression pattern. For activated CD4+ T cells, the TF network contained 17,285 nodes (genes) and 211,108 edges; signaling network included 15,370 nodes (genes) and 214,971 edges. After Identity Documen (ID) conversion and combining these two networks, the final data-driven activated CD4+ T cell interactome (CD4Ti) consisted of 17,451 nodes (genes) and 426,079 edges, among which there were 7445 unique driver candidates, including 1557 transcriptional factors and 5888 signaling molecules. For activated CD8+ T cells, the final CD8+ T cell interactome (CD8Ti) consisted of 12,938 nodes and 646,947 edges, among which there were 6903 unique driver candidates, including 1294 transcriptional factors and 5609 signaling molecules. For tumor cells, the final interactome (Tumori) consisted of 22,394 nodes and 314,914 edges, of which there were 10,843 unique hub genes (1937 transcriptional factors and 8906 signaling molecules). Then, we used the cal.Activity function (method = "weightedmean") in NetBID to infer the activities of driver genes for each cell from their respective gene expression profiles and the transformed Tumori, CD4Ti, and CD8Ti. The weighted mean activity of a driver candidate gene (DRIVER) i in sample s

was defined by the following equation

$$\text{DRIVER}_{si} = \frac{\sum_{j=1}^{n} \text{SIGN}_{ij} * \text{MI}_{ij} * \text{EXP}_{sj}}{n}$$

The gene expression matrix was z-normalized in each sample, and EXP_{sj} is the expression value of gene j in sample s. MI_{ij} is the mutual information between master regulator gene i and its target gene j, and SIGN_{ij} is the sign of Spearman correlation between gene i and its target gene j. The total number of targets for DRIVER i is denoted by n. To identify differentially regulated genes in blinatumomab-sensitive and blinatumomab-resistant cell lines, differential activities of two comparisons (sensitive cases versus resistance cases) were calculated by NetBID function "getDE.BID.2G." We also performed pathway analysis to identify the enrichment of drivers in specific biological processes by querying the Molecular Signatures Database pathway database and evaluating the statistical significance of enrichment by NetBID function getDE.BID.2G.

Supplementary Materials
This PDF file includes:
Figs. S1 to S17
Tables S1 to S5

View/request a protocol for this paper from *Bio-protocol*.

REFERENCES AND NOTES
1. F. Locatelli, G. Zugmaier, C. Rizzari, J. D. Morris, B. Gruhn, T. Klingebiel, R. Parasole, C. Linderkamp, C. Flotho, A. Petit, C. Micalizzi, N. Mergen, A. Mohammad, W. N. Kormany, C. Eckert, A. Möricke, M. Sartor, O. Hrusak, C. Peters, V. Saha, L. Vinti, A. von Stackelberg, Effect of blinatumomab vs chemotherapy on event-free survival among children with high-risk first-relapse B-cell acute lymphoblastic leukemia: A randomized clinical trial. *JAMA* **325**, 843–854 (2021).
2. A. Löffler, P. Kufer, R. Lutterbüse, F. Zettl, P. T. Daniel, J. M. Schwenkenbecher, G. Riethmüller, B. Dörken, R. C. Bargou, A recombinant bispecific single-chain antibody, CD19 x CD3, induces rapid and high lymphoma-directed cytotoxicity by unstimulated T lymphocytes. *Blood* **95**, 2098–2103 (2000).
3. Y. Huo, Z. Sheng, D. R. Lu, D. C. Ellwanger, C.-M. Li, O. Homann, S. Wang, H. Yin, R. Ren, Blinatumomab-induced T cell activation at single cell transcriptome resolution. *BMC Genomics* **22**, 145 (2021).
4. P. Hoffmann, R. Hofmeister, K. Brischwein, C. Brandl, S. Crommer, R. Bargou, C. Itin, N. Prang, P. A. Baeuerle, Serial killing of tumor cells by cytotoxic T cells redirected with a CD19-/CD3-bispecific single-chain antibody construct. *Int. J. Cancer* **115**, 98–104 (2005).
5. P. A. Brown, L. Ji, X. Xu, M. Devidas, L. E. Hogan, M. J. Borowitz, E. A. Raetz, G. Zugmaier, E. Sharon, M. B. Bernhardt, S. A. Terezakis, L. Gore, J. A. Whitlock, M. A. Pulsipher, S. P. Hunger, M. L. Loh, Effect of postreinduction therapy consolidation with blinatumomab vs chemotherapy on disease-free survival in children, adolescents, and young adults with first relapse of B-cell acute lymphoblastic leukemia: A randomized clinical trial. *JAMA* **325**, 833–842 (2021).
6. H. Kantarjian, A. Stein, N. Gökbuget, A. K. Fielding, A. C. Schuh, J. M. Ribera, A. Wei, H. Dombret, R. Foà, R. Bassan, Ö. Arslan, M. A. Sanz, J. Bergeron, F. Demirkan, E. Lech-Maranda, A. Rambaldi, X. Thomas, H. A. Horst, M. Brüggemann, W. Klapper, B. L. Wood, A. Fleishman, D. Nagorsen, C. Holland, Z. Zimmerman, M. S. Topp, Blinatumomab versus chemotherapy for advanced acute lymphoblastic leukemia. *N. Engl. J. Med.* **376**, 836–847 (2017).
7. M. S. Topp, N. Gökbuget, A. S. Stein, G. Zugmaier, S. O'Brien, R. C. Bargou, H. Dombret, A. K. Fielding, L. Heffner, R. A. Larson, S. Neumann, R. Foà, M. Litzow, J.-M. Ribera, A. Rambaldi, G. Schiller, M. Brüggemann, H. A. Horst, C. Holland, C. Jia, T. Maniar, B. Huber, D. Nagorsen, S. J. Forman, H. M. Kantarjian, Safety and activity of blinatumomab for adult patients with relapsed or refractory B-precursor acute lymphoblastic leukaemia: A multicentre, single-arm, phase 2 study. *Lancet Oncol.* **16**, 57–66 (2015).
8. A. S. Stein, H. Kantarjian, N. Gökbuget, R. Bargou, M. R. Litzow, A. Rambaldi, J.-M. Ribera, A. Zhang, Z. Zimmerman, G. Zugmaier, M. S. Topp, Blinatumomab for acute lymphoblastic leukemia relapse after allogeneic hematopoietic stem cell transplantation. *Biol. Blood Marrow Transplant.* **25**, 1498–1504 (2019).

9. T. Badar, A. Szabo, A. Advani, M. Wadleigh, S. Arslan, M. A. Khan, I. Aldoss, C. Siebenaller, E. Schultz, M. Hefazi, R. M. Shallis, I. Yurkiewicz, N. Podoltsev, A. A. Patel, E. Curran, S. Balasubramanian, J. Yang, R. J. Mattison, M. Burkart, S. Dinner, M. Liedtke, M. R. Litzow, E. Atallah, Real-world outcomes of adult B-cell acute lymphocytic leukemia patients treated with blinatumomab. *Blood Adv.* **4**, 2308–2316 (2020).

10. K. Wudhikarn, A. C. King, M. B. Geyer, M. Roshal, Y. Bernal, B. Gyurkocza, M.-A. Perales, J. H. Park, Outcomes of relapsed B-cell acute lymphoblastic leukemia after sequential treatment with blinatumomab and inotuzumab. *Blood Adv.* **6**, 1432–1443 (2022).

11. N. Gökbuget, G. Zugmaier, M. Klinger, P. Kufer, M. Stelljes, A. Viardot, H. A. Horst, S. Neumann, M. Brüggemann, O. G. Ottmann, T. Burmeister, D. Wessiepe, M. S. Topp, R. Bargou, Long-term relapse-free survival in a phase 2 study of blinatumomab for the treatment of patients with minimal residual disease in B-lineage acute lymphoblastic leukemia. *Haematologica* **102**, e132–e135 (2017).

12. M. S. Topp, P. Kufer, N. Gökbuget, M. Goebeler, M. Klinger, S. Neumann, H. A. Horst, T. Raff, A. Viardot, M. Schmid, M. Stelljes, M. Schaich, E. Degenhard, R. Köhne-Volland, M. Brüggemann, O. Ottmann, H. Pfeifer, T. Burmeister, D. Nagorsen, M. Schmidt, R. Lutterbuese, C. Reinhardt, P. A. Baeuerle, M. Kneba, H. Einsele, G. Riethmüller, D. Hoelzer, G. Zugmaier, R. C. Bargou, Targeted therapy with the T-cell-engaging antibody blinatumomab of chemotherapy-refractory minimal residual disease in B-lineage acute lymphoblastic leukemia patients results in high response rate and prolonged leukemia-free survival. *J. Clin. Oncol.* **29**, 2493–2498 (2011).

13. E. Y. Jen, Q. Xu, A. Schetter, D. Przepiorka, Y. L. Shen, D. Roscoe, R. Sridhara, A. Deisseroth, R. Philip, A. T. Farrell, R. Pazdur, FDA approval: Blinatumomab for patients with B-cell precursor acute lymphoblastic leukemia in morphologic remission with minimal residual disease. *Clin. Cancer Res.* **25**, 473–477 (2019).

14. N. Gökbuget, H. Dombret, M. Bonifacio, A. Reichle, C. Graux, C. Faul, H. Diedrich, M. S. Topp, M. Brüggemann, H.-A. Horst, V. Havelange, J. Stieglmaier, H. Wessels, V. Haddad, J. E. Benjamin, G. Zugmaier, D. Nagorsen, R. C. Bargou, Blinatumomab for minimal residual disease in adults with B-cell precursor acute lymphoblastic leukemia. *Blood* **131**, 1522–1531 (2018).

15. R. Foà, R. Bassan, A. Vitale, L. Elia, A. Piciocchi, M.-C. Puzzolo, M. Canichella, P. Viero, F. Ferrara, M. Lunghi, F. Fabbiano, M. Bonifacio, N. Fracchiolla, P. D. Bartolomeo, A. Mancino, M.-S. De Propris, M. Vignetti, A. Guarini, A. Rambaldi, S. Chiaretti; GIMEMA Investigators, Dasatinib-blinatumomab for Ph-positive acute lymphoblastic leukemia in adults. *N. Engl. J. Med.* **383**, 1613–1623 (2020).

16. N. J. Short, H. Kantarjian, E. Jabbour, Optimizing the treatment of acute lymphoblastic leukemia in younger and older adults: New drugs and evolving paradigms. *Leukemia* **35**, 3044–3058 (2021).

17. E. J. Jabbour, K. Sasaki, F. Ravandi, N. J. Short, G. Garcia-Manero, N. Daver, T. Kadia, M. Konopleva, N. Jain, J. Cortes, G. C. Issa, J. Jacob, M. Kwari, P. Thompson, R. Garris, N. Pemmaraju, M. Yilmaz, S. M. O'Brien, H. M. Kantarjian, Inotuzumab ozogamicin in combination with low-intensity chemotherapy (mini-HCVD) with or without blinatumomab versus standard intensive chemotherapy (HCVAD) as frontline therapy for older patients with Philadelphia chromosome–negative acute lymphoblastic leukemia: A propensity score analysis. *Cancer* **125**, 2579–2586 (2019).

18. N. Short, H. Kantarjian, M. Konopleva, N. Jain, F. Ravandi, X. Huang, W. Macaron, W. Wierda, G. Borthakur, T. Kadia, K. Sasaki, G. Issa, G. Montalban-Bravo, Y. Alvarado, G. Garcia-Manero, C. Dinardo, J. Thankachan, R. Delumpa, E. Mayor, W. Deen, A. Milton, J. Rivera, L. Waller, C. Loiselle, R. Garris, E. Jabbour, Combination of ponatinib and blinatumomab in Philadelphia chromosome-positive acute lymphoblastic leukemia: Early results from a phase II study. Paper presented at the ASCO Annual Meeting I, Fri, Jun 4, 2021, online.

19. L. Gore, F. Locatelli, G. Zugmaier, R. Handgretinger, M. M. O'Brien, P. Bader, D. Bhojwani, P. G. Schlegel, C. A. Tuglus, A. von Stackelberg, Survival after blinatumomab treatment in pediatric patients with relapsed/refractory B-cell precursor acute lymphoblastic leukemia. *Blood Cancer J.* **8**, 80 (2018).

20. A. von Stackelberg, F. Locatelli, G. Zugmaier, R. Handgretinger, T. M. Trippett, C. Rizzari, P. Bader, M. M. O'Brien, B. Brethon, D. Bhojwani, P. G. Schlegel, A. Borkhardt, S. R. Rheingold, T. M. Cooper, C. M. Zwaan, P. Barnette, C. Messina, G. Michel, S. G. DuBois, K. Hu, M. Zhu, J. A. Whitlock, L. Gore, Phase I/phase II study of blinatumomab in pediatric patients with relapsed/refractory acute lymphoblastic leukemia. *J. Clin. Oncol.* **34**, 4381–4389 (2016).

21. N. Gökbuget, M. Kelsh, V. Chia, A. Advani, R. Bassan, H. Dombret, M. Doubek, A. K. Fielding, S. Giebel, V. Haddad, D. Hoelzer, C. Holland, N. Ifrah, A. Katz, T. Maniar, G. Martinelli, M. Morgades, S. O'Brien, J.-M. Ribera, J. M. Rowe, A. Stein, M. Topp, M. Wadleigh, H. Kantarjian, Blinatumomab vs historical standard therapy of adult relapsed/refractory acute lymphoblastic leukemia. *Blood Cancer J.* **6**, e473 (2016).

22. A. S. Advani, A. Moseley, K. M. O'Dwyer, B. L. Wood, M. Fang, M. J. Wieduwilt, I. Aldoss, J. H. Park, R. B. Klisovic, M. R. Baer, W. Stock, R. R. Bhave, R. C. Harvey, C. L. Willman, M. R. Litzow, R. M. Stone, E. Sharon, H. P. Erba, SWOG 1318: A phase II trial of blinatumomab followed by POMP maintenance in older patients with newly diagnosed philadelphia chromosome-negative B-cell acute lymphoblastic leukemia. *J. Clin. Oncol.* **40**, 1574–1582 (2022).

23. Y. Zhao, I. Aldoss, C. Qu, J. C. Crawford, Z. Gu, E. K. Allen, A. E. Zamora, T. B. Alexander, J. Wang, H. Goto, T. Imamura, K. Akahane, G. Marcucci, A. S. Stein, R. Bhatia, P. G. Thomas, S. J. Forman, C. G. Mullighan, K. G. Roberts, Tumor-intrinsic and -extrinsic determinants of response to blinatumomab in adults with B-ALL. *Blood* **137**, 471–484 (2021).

24. T. Köhnke, C. Krupka, J. Tischer, T. Knosel, M. Subklewe, Increase of PD-L1 expressing B-precursor ALL cells in a patient resistant to the CD19/CD3-bispecific T cell engager antibody blinatumomab. *J. Hematol. Oncol.* **8**, 111 (2015).

25. F. Braig, A. Brandt, M. Goebeler, H. P. Tony, A.-K. Kurze, P. Nollau, T. Bumm, S. Böttcher, R. C. Bargou, M. Binder, Resistance to anti-CD19/CD3 BiTE in acute lymphoblastic leukemia may be mediated by disrupted CD19 membrane trafficking. *Blood* **129**, 100–104 (2017).

26. J. Duell, M. Dittrich, T. Bedke, T. Mueller, F. Eisele, A. Rosenwald, L. Rasche, E. Hartmann, T. Dandekar, H. Einsele, M. S. Topp, Frequency of regulatory T cells determines the outcome of the T-cell-engaging antibody blinatumomab in patients with B-precursor ALL. *Leukemia* **31**, 2181–2190 (2017).

27. M. C. van Zelm, J. Smet, B. Adams, F. Mascart, L. Schandené, F. Janssen, A. Ferster, C.-C. Kuo, S. Levy, J. J. M. van Dongen, M. van der Burg, CD81 gene defect in humans disrupts CD19 complex formation and leads to antibody deficiency. *J. Clin. Invest.* **120**, 1265–1274 (2010).

28. J. A. Gollob, J. Li, H. Kawasaki, J. F. Daley, C. Groves, E. L. Reinherz, J. Ritz, Molecular interaction between CD58 and CD2 counter-receptors mediates the ability of monocytes to augment T cell activation by IL-12. *J. Immunol.* **157**, 1886–1893 (1996).

29. P. Selvaraj, M. L. Plunkett, M. Dustin, M. E. Sanders, S. Shaw, T. A. Springer, The T lymphocyte glycoprotein CD2 binds the cell surface ligand LFA-3. *Nature* **326**, 400–403 (1987).

30. H. Zhang, Y. Zhang, X. Zhou, S. Wright, J. Hyle, L. Zhao, J. An, X. Zhao, Y. Shao, B. Xu, H.-M. Lee, T. Chen, Y. Zhou, X. Chen, R. Lu, C. Li, Functional interrogation of HOXA9 regulome in MLLr leukemia via reporter-based CRISPR/Cas9 screen. *eLife* **9**, e57858 (2020).

31. Z. Gu, M. L. Churchman, K. G. Roberts, I. Moore, X. Zhou, J. Nakitandwe, K. Hagiwara, S. Pelletier, S. Gingras, H. Berns, D. Payne-Turner, A. Hill, I. Iacobucci, L. Shi, S. Pounds, C. Cheng, D. Pei, C. Qu, S. Newman, M. Devidas, Y. Dai, S. C. Reshmi, J. Gastier-Foster, E. A. Raetz, M. J. Borowitz, B. L. Wood, W. L. Carroll, P. A. Zweidler-Mc Kay, K. R. Rabin, L. A. Mattano, K. W. Maloney, A. Rambaldi, O. Spinelli, J. P. Radich, M. D. Minden, J. M. Rowe, S. Luger, M. R. Litzow, M. S. Tallman, J. Racevskis, Y. Zhang, R. Bhatia, J. Kohlschmidt, K. Mrózek, C. D. Bloomfield, W. Stock, S. Kornblau, H. M. Kantarjian, M. Konopleva, W. E. Evans, S. Jeha, C.-H. Pui, J. Yang, E. Paietta, J. R. Downing, M. V. Relling, J. Zhang, M. L. Loh, S. P. Hunger, C. G. Mullighan, PAX5-driven subtypes of B-progenitor acute lymphoblastic leukemia. *Nat. Genet.* **51**, 296–307 (2019).

32. M. T. Witkowski, S. Lee, E. Wang, A. K. Lee, A. Talbot, C. Ma, N. Tsopoulidis, J. Brumbaugh, Y. Zhao, K. G. Roberts, S. J. Hogg, S. Nomikou, Y. E. Ghebrechristos, P. Thandapani, C. G. Mullighan, K. Hochedlinger, W. Chen, O. Abdel-Wahab, J. Eyquem, I. Aifantis, NUDT21 limits CD19 levels through alternative mRNA polyadenylation in B cell acute lymphoblastic leukemia. *Nat. Immunol.* **23**, 1424–1432 (2022).

33. R. Wallich, C. Brenner, Y. Brand, M. Roux, M. Reister, S. Meuer, Gene structure, promoter characterization, and basis for alternative mRNA splicing of the human CD58 gene. *J. Immunol.* **160**, 2862–2871 (1998).

34. M. Challa-Malladi, Y. K. Lieu, O. Califano, A. B. Holmes, G. Bhagat, V. V. Murty, D. Dominguez-Sola, L. Pasqualucci, R. Dalla-Favera, Combined genetic inactivation of β2-microglobulin and CD58 reveals frequent escape from immune recognition in diffuse large B cell lymphoma. *Cancer Cell* **20**, 728–740 (2011).

35. F. R. Abdul Razak, A. Diepstra, L. Visser, A. van den Berg, CD58 mutations are common in Hodgkin lymphoma cell lines and loss of CD58 expression in tumor cells occurs in Hodgkin lymphoma patients who relapse. *Genes Immun.* **17**, 363–366 (2016).

36. X. Yan, D. Chen, X. Ma, Y. Wang, Y. Guo, J. Wei, C. Tong, Q. Zhu, Y. Lu, Y. Yu, Z. Wu, W. Han, CD58 loss in tumor cells confers functional impairment of CAR T cells. *Blood Adv.* **6**, 5844–5856 (2022).

37. R. Majzner, M. Frank, C. W. Mount, A. Tousley, D. Kurtz, B. Sworder, K. Murphy, A. Manousopoulou, K. Kohler, M. Rotiroti, J. Spiegel, Y. Natkunam, S. Younes, E. Sotillo, V.-A. Duong, C. Macaulay, Z. Good, P. Xu, L. Labanieh, L. D. Wang, A. A. Alizadeh, M. Monje, D. Miklos, C. Mackall, CD58 aberrations limit durable responses to CD19 CAR in large B cell lymphoma patients treated with axicabtagene ciloleucel but can be overcome through novel CAR engineering. *Blood* **136**, 53–54 (2020).

38. S. P. Hunger, C. G. Mullighan, Acute lymphoblastic leukemia in children. *N. Engl. J. Med.* **373**, 1541–1552 (2015).

39. I. Iacobucci, C. G. Mullighan, Genetic basis of acute lymphoblastic leukemia. *J. Clin. Oncol.* **35**, 975–983 (2017).

40. Z. Kozmik, S. Wang, P. Dorfler, B. Adams, M. Busslinger, The promoter of the CD19 gene is a target for the B-cell-specific transcription factor BSAP. *Mol. Cell. Biol.* **12**, 2662–2672 (1992).

41. S. Wang, K. Chen, Q. Lei, P. Ma, A. Q. Yuan, Y. Zhao, Y. Jiang, H. Fang, S. Xing, Y. Fang, N. Jiang, H. Miao, M. Zhang, S. Sun, Z. Yu, W. Tao, Q. Zhu, Y. Nie, N. Li, The state of the art of bispecific antibodies for treating human malignancies. *EMBO Mol. Med.* **13**, e14291 (2021).

42. M. Bacac, S. Colombetti, S. Herter, J. Sam, M. Perro, S. Chen, R. Bianchi, A. Schoenle, V. Nicolini, S. Diggelmann, F. Limani, R. Schlenker, T. Hüsser, W. Richter, K. Bray-French, H. Hinton, A. M. Giusti, A. Freimoser-Grundschober, L. Lariviere, C. Neumann, C. Klein, P. Umaña, CD20-TCB with obinutuzumab pretreatment as next-generation treatment of hematologic malignancies. *Clin. Cancer Res.* **24**, 4785–4797 (2018).

43. L. E. Budde, S. Assouline, L. H. Sehn, S. J. Schuster, S.-S. Yoon, D. H. Yoon, M. J. Matasar, F. Bosch, W. S. Kim, L. J. Nastoupil, I. W. Flinn, M. Shadman, C. Diefenbach, C. O'Hear, H. Huang, A. Kwan, C.-C. Li, E. C. Piccione, M. C. Wei, S. Yin, N. L. Bartlett, Single-agent mosunetuzumab shows durable complete responses in patients with relapsed or refractory B-cell lymphomas: Phase I dose-escalation study. *J. Clin. Oncol.* **40**, 481–491 (2022).

44. T. J. Phillips, A. J. Olszewski, J. Munoz, T. M. Kim, D. H. Yoon, R. Greil, J. Westin, U. Jaeger, M. Canales, C. Chen, B. Althaus, C. O'Hear, R. Negricea, Y. Xie, R. M. Cord, E. Purev, A. Vallurupalli, Mosunetuzumab, a novel CD20/CD3 bispecific antibody, in combination with CHOP confers high response rates in patients with diffuse large B-cell lymphoma. *Blood* **136**, 37–38 (2022).

45. R. Bannerji, J. N. Allan, J. E. Arnason, J. R. Brown, R. Advani, S. M. Ansell, S. M. O'Brien, J. Duell, P. Martin, R. M. Joyce, J. Li, D. M. Flink, M. Zhu, D. M. Weinreich, G. D. Yancopoulos, A. Sirulnik, A. Chaudhry, S. R. Ambati, M. S. Topp, Odronextamab (REGN1979), a human CD20 x CD3 bispecific antibody, induces durable, complete responses in patients with highly refractory B-cell non-Hodgkin lymphoma, including patients refractory to CAR T therapy. *Blood* **136**, 42–43 (2020).

46. M. Hutchings, C. Carlo-Stella, E. Bachy, F. C. Offner, F. Morschhauser, M. Crump, G. Iacoboni, A. S. Balari, J. Martinez-Lopez, L. Lundberg, M. Dixon, D. P. Callejo, J. Relf, D. Carlile, E. Piccione, K. Humphrey, M. Dickinson, Glofitamab step-up dosing induces high response rates in patients with hard-to-treat refractory or relapsed non-Hodgkin lymphoma. *Blood* **136**, 46–48 (2020).

47. N. N. Shah, L. Sokol, Targeting CD22 for the treatment of B-cell malignancies. *Immunotargets Ther.* **10**, 225–236 (2021).

48. Y. Shen, J. S. Eng, F. Fajardo, L. Liang, C. Li, P. Collins, D. Tedesco, O. Nolan-Stevaux, Cancer cell-intrinsic resistance to BiTE therapy is mediated by loss of CD58 costimulation and modulation of the extrinsic apoptotic pathway. *J. Immunother. Cancer* **10**, e004348 (2022).

49. Y. Gocho, J. Liu, J. Hu, W. Yang, N. V. Dharia, J. Zhang, H. Shi, G. du, A. John, T.-N. Lin, J. Hunt, X. Huang, B. Ju, L. Rowland, L. Shi, D. Maxwell, B. Smart, K. R. Crews, W. Yang, K. Hagiwara, Y. Zhang, K. Roberts, H. Wang, E. Jabbour, W. Stock, B. Eisfelder, E. Paietta, S. Newman, G. Roti, M. Litzow, J. Easton, J. Zhang, J. Peng, H. Chi, S. Pounds, M. V. Relling, H. Inaba, X. Zhu, S. Kornblau, C.-H. Pui, M. Konopleva, D. Teachey, C. G. Mullighan, K. Stegmaier, W. E. Evans, J. Yu, J. J. Yang, Network-based systems pharmacology reveals heterogeneity in LCK and BCL2 signaling and therapeutic sensitivity of T-cell acute lymphoblastic leukemia. *Nat. Cancer* **2**, 284–299 (2021).

50. N. E. Sanjana, O. Shalem, F. Zhang, Improved vectors and genome-wide libraries for CRISPR screening. *Nat. Methods* **11**, 783–784 (2014).

51. R. J. Autry, S. W. Paugh, R. Carter, L. Shi, J. Liu, D. C. Ferguson, C. E. Lau, E. J. Bonten, W. Yang, J. R. McCorkle, J. A. Beard, J. C. Panetta, J. D. Diedrich, K. R. Crews, D. Pei, C. J. Coke, S. Natarajan, A. Khatamian, S. E. Karol, E. Lopez-Lopez, B. Diouf, C. Smith, Y. Gocho, K. Hagiwara, K. G. Roberts, S. Pounds, S. M. Kornblau, W. Stock, E. M. Paietta, M. R. Litzow, H. Inaba, C. G. Mullighan, S. Jeha, C. H. Pui, C. Cheng, D. Savic, J. Yu, C. Gawad, M. V. Relling, J. J. Yang, W. E. Evans, Integrative genomic analyses reveal mechanisms of glucocorticoid resistance in acute lymphoblastic leukemia. *Nat. Cancer* **1**, 329–344 (2020).

52. O. Shalem, N. E. Sanjana, E. Hartenian, X. Shi, D. A. Scott, T. S. Mikkelsen, D. Heckl, B. L. Ebert, D. E. Root, J. G. Doench, F. Zhang, Genome-scale CRISPR-Cas9 knockout screening in human cells. *Science* **343**, 84–87 (2014).

53. W. Li, J. Köster, H. Xu, C.-H. Chen, T. Xiao, J. S. Liu, M. Brown, X. S. Liu, Quality control, modeling, and visualization of CRISPR screens with MAGeCK-VISPR. *Genome Biol.* **16**, 281 (2015).

54. Y. Li, W. Yang, M. Devidas, S. S. Winter, C. Kesserwan, W. Yang, K. P. Dunsmore, C. Smith, M. Qian, X. Zhao, R. Zhang, J. M. Gastier-Foster, E. A. Raetz, W. L. Carroll, C. Li, P. P. Liu, K. R. Rabin, T. Sanda, C. G. Mullighan, K. E. Nichols, W. E. Evans, C.-H. Pui, S. P. Hunger, D. T. Teachey, M. V. Relling, M. L. Loh, J. J. Yang, Germline RUNX1 variation and predisposition to childhood acute lymphoblastic leukemia. *J. Clin. Invest.* **131**, e147898 (2021).

55. A. Dobin, C. A. Davis, F. Schlesinger, J. Drenkow, C. Zaleski, S. Jha, P. Batut, M. Chaisson, T. R. Gingeras, STAR: Ultrafast universal RNA-seq aligner. *Bioinformatics* **29**, 15–21 (2013).

56. J. Harrow, A. Frankish, J. M. Gonzalez, E. Tapanari, M. Diekhans, F. Kokocinski, B. L. Aken, D. Barrell, A. Zadissa, S. Searle, I. Barnes, A. Bignell, V. Boychenko, T. Hunt, M. Kay, G. Mukherjee, J. Rajan, G. Despacio-Reyes, G. Saunders, C. Steward, R. Harte, M. Lin, C. Howald, A. Tanzer, T. Derrien, J. Chrast, N. Walters, S. Balasubramanian, B. Pei, M. Tress, J. M. Rodriguez, I. Ezkurdia, J. van Baren, M. Brent, D. Haussler, M. Kellis, A. Valencia, A. Reymond, M. Gerstein, R. Guigó, T. J. Hubbard, GENCODE: The reference human genome annotation for The ENCODE Project. *Genome Res.* **22**, 1760–1774 (2012).

57. A. Frankish, M. Diekhans, A. M. Ferreira, R. Johnson, I. Jungreis, J. Loveland, J. M. Mudge, C. Sisu, J. Wright, J. Armstrong, I. Barnes, GENCODE reference annotation for the human and mouse genomes. *Nucleic Acids Res.* **47**, D766–D773 (2018).

58. M. D. Robinson, D. J. McCarthy, G. K. Smyth, edgeR: A Bioconductor package for differential expression analysis of digital gene expression data. *Bioinformatics* **26**, 139–140 (2010).

59. D. J. McCarthy, Y. Chen, G. K. Smyth, Differential expression analysis of multifactor RNA-Seq experiments with respect to biological variation. *Nucleic Acids Res.* **40**, 4288–4297 (2012).

60. Y. Chen, A. T. Lun, G. K. Smyth, From reads to genes to pathways: Differential expression analysis of RNA-Seq experiments using Rsubread and the edgeR quasi-likelihood pipeline. *F1000Res* **5**, 1438 (2016).

61. B. J. Quah, H. S. Warren, C. R. Parish, Monitoring lymphocyte proliferation in vitro and in vivo with the intracellular fluorescent dye carboxyfluorescein diacetate succinimidyl ester. *Nat. Protoc.* **2**, 2049–2056 (2007).

62. M. R. Corces, J. D. Buenrostro, B. Wu, P. G. Greenside, S. M. Chan, J. L. Koenig, M. P. Snyder, J. K. Pritchard, A. Kundaje, W. J. Greenleaf, R. Majeti, H. Y. Chang, Lineage-specific and single-cell chromatin accessibility charts human hematopoiesis and leukemia evolution. *Nat. Genet.* **48**, 1193–1203 (2016).

63. T. Stuart, A. Butler, P. Hoffman, C. Hafemeister, E. Papalexi, W. M. Mauck III, Y. Hao, M. Stoeckius, P. Smibert, R. Satija, Comprehensive integration of single-cell data. *Cell* **177**, 1888–1902.e21 (2019).

64. X. Du, J. Wen, Y. Wang, P. W. F. Karmaus, A. Khatamian, H. Tan, Y. Li, C. Guy, T.-L. M. Nguyen, Y. Dhungana, G. Neale, J. Peng, J. Yu, H. Chi, Hippo/Mst signalling couples metabolic state and immune function of CD8α⁺ dendritic cells. *Nature* **558**, 141–145 (2018).

65. A. Khatamian, E. O. Paull, A. Califano, J. Y. Yu, SJARACNe: A scalable software tool for gene network reverse engineering from big data. *Bioinformatics* **35**, 2165–2166 (2019).